Earthworms in an enhanced weathering mesocosm experiment: effects on soil carbon sequestration, base cation exchange and soil CO_2 efflux.

Arthur Vienne[1], Patrick Frings[1, 2] Silvia Poblador[1], Laura Steinwidder[1], Jet Rijnders[1], Jonas Schoelynck[3], Olga Vinduskova[1], Sara Vicca[1]

1 PLECO (Plants and Ecosystems), Department of Biology, University of Antwerp, Antwerp, Belgium
2 GFZ German Research Centre for Geosciences, Section Earth Surface Geochemistry, Telegrafenberg, 14473 Potsdam, Germany
3 ECOSPHERE, Department of Biology, University of Antwerp, Antwerp, Belgium

Corresponding author: *Arthur Vienne[1]* (arthur.vienne@uantwerpen.be) Universiteitsplein 1, 2610 Wilrijk, Belgium
Keywords: Enhanced weathering, Basalt, CDR, earthworms, SCE, SOC, base cation exchange

Highlights:

- **Base cation exchange increased after basalt amendment and prevented substantial DIC leaching from basalt mesocosms.**
- **Base cation exchange was stimulated by earthworms in basalt mesocosms.**
- **Soil exchangeable cations increased in basalt treatments and indicated a log minimal weathering rate of -11.65 mol alkalinity m^{-2} s^{-1}.**
- **In this experiment, we calculated inorganic carbon dioxide removal (CDR) equivalents of 0.62-1.09 ton CO_2/ha or 0.017-0.029 ton CO_2 ton $basalt^{-1}$ $year^{-1}$.**
- **Soil CO_2 efflux did not decrease in all basalt treatments, indicating that basalt amendment affected soil organic carbon fluxes.**

Graphical abstract

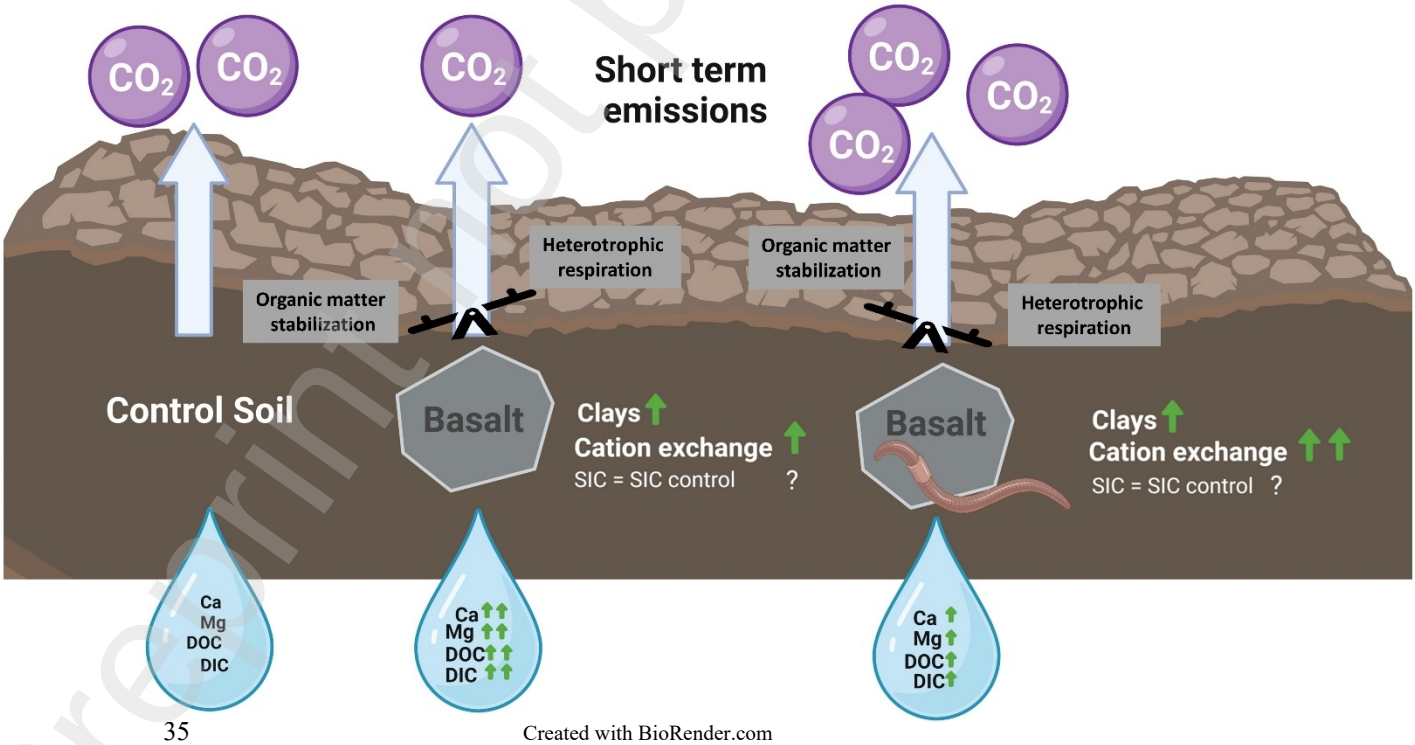

Created with BioRender.com

Abstract

Virtually all scenarios that limit global warming to 1.5°C require large scale carbon dioxide removal (CDR). Enhanced weathering (EW) is considered an attractive CDR technology because of the permanence of sequestered inorganic carbon and its scalability. Yet, a great challenge in EW research is the quantification of weathering and C sequestration rates. In addition, soil (macro)biota such as earthworms were postulated to stimulate silicate dissolution, but quantitative data on how earthworms influence (in)organic C sequestration in EW systems are lacking. To evaluate the effect of earthworms on EW, we set up a 4.5 months mesocosm experiment with the following treatments: control soil, soil with basalt (100 ton ha^{-1}), soil with earthworms and soil with both basalt and earthworms.

Basalt increased cumulative dissolved inorganic carbon export by only 40 kg CO_2 ha^{-1}. Using a novel Ge/Si and $\delta^{30}Si$ monitoring technique we found qualitative proof of mineral weathering and secondary clay formation. From the large increase in exchanged base cations we could calculate a minimal basalt weathering rate of over 10^{-12} mol total alkalinity m^{-2} s^{-1}, which is within the range observed in other basalt EW experiments that quantified base cations in the exchangeable pool. In this specific experiment, soil CO_2 efflux (SCE) decreased after basalt amendment, but only in non-worm soils.

Earthworms decreased dissolved inorganic C export and no earthworm-induced increase in soil inorganic C sequestration was observed. Instead, earthworms were found to enlarge clay precipitation and base cation exchange, increasing the basalt weathering rate and inorganic CDR equivalents. Within this short-term experiment however, earthworm activity increased SCE more in basalt than in control mesocosms, suggesting stimulation of earthworm microbiota through EW. In conclusion, earthworms did not cause net CDR within this short experimental timeframe, but they stimulated basalt dissolution with potential benefits for organic matter stability in the long run.

Introduction

Virtually all scenarios that limit global warming to 1.5°C require large scale carbon dioxide removal (CDR) (IPCC, 2021). Enhanced Weathering (EW) is a potentially important CDR technology, underpinned by the same mechanism that consumes CO_2 during 'natural' weathering of silicate rocks, which has regulated Earth's climate over geological timescales (Berner, 2004). Silicate weathering by carbonic acid (H_2CO_3) (illustrated for the mineral forsterite (Mg_2SiO_4) in Reaction 1) produces 2 moles of HCO_3^- for every divalent cation liberated from silicate minerals. The HCO_3^- can remain in solution as dissolved inorganic carbon (DIC), or can recombine with base cations to form a carbonate mineral (in soils or in catchments). For every two moles of HCO_3^-, the latter re-releases 1 mole of CO_2 (Reaction 2) while 1 mole of C is sequestered as soil inorganic carbon (SIC). Both the DIC and SIC sequestration pathways trap CO_2 for thousands of years, forming a stable carbon sink if no acid is added to the system, which would degas the produced (bi)carbonates again (Berner 2004). The idea behind EW is to accelerate Reaction 1 by grinding and distributing silicate rock, vastly increasing reactive surface areas in CO_2-rich soils, and therefore CO_2 consumption rates (Schuiling & Krijgsman, 2006).

$$Mg_2SiO_4 + 4CO_2 + 4H2O \rightarrow 2Mg^{2+}\ 4HCO_3^- + H_4SiO_4 \qquad \textbf{Reaction 1}$$

$$Ca^{2+} + Mg^{2+} + 4HCO_3^- \rightarrow MgCa(CO_3)_2 + 2CO_2 + 2H_2O \qquad \textbf{Reaction 2}$$

During weathering, cations are released, as illustrated in Reactions 1 and 2 for forsterite, one of the minerals present in basalt. Free base cations (Mg^{2+} and Ca^{2+}) can oversaturate to form a carbonate, dolomite ($MgCa(CO_3)_2$) in this case. In reaction 2, 50% of the sequestered HCO_3^- molecules (generated in weathering reactions 1) are degassed to CO_2 again.

Although theoretically more inorganic C can be sequestered per unit of rock for olivine (or dunite rock which mostly contains olivine) than for basalt, olivine is more concentrated in Ni and Cr than basalt. Therefore, agricultural

EW studies focus on basalt rather than olivine amendment (Beerling et al., 2018).

Recently, soil (macro)biota were postulated to have a potentially large influence on (enhanced) weathering in soils (Dorn, 2014; Gerrits et al., 2020; Rosenstock et al.,2019; Verbruggen et al., 2021; Vicca et al., 2022; Wild et al., 2022). Earthworms are the most abundant animal component of the soil biomass and are seen as 'ecosystem engineers' due to their considerable impact on the soil environment. They have a diversity of lifestyles, and can be classified as a function of their tunnelling behaviour. For example, anecic earthworms (e.g. *Lumbricus terrestris* Linnaeus, 1758) feed on litter in the topsoil and generate vertical burrows up to 3 m depth (Wen et al., 2022), while endogeic earthworms (e.g. *Aporrectodea caliginosa* Savigny, 1826) feed and live in the mineral soil layer (soil dwellers) while tunnelling horizontally (Huang et al., 2020). For example, they alter soil structure, contribute to soil formation and nutrient cycling, and regulate soil water pools and fluxes (Blouin et al., 2013). Earthworms have been suggested to accelerate mineral dissolution physically and chemically (Carpenter et al., 2007), but these mechanisms are yet to be unraveled (Blouin et al., 2013; Liu et al., 2011).

Potential physical mechanisms might include the breakdown of silicate grains (increasing exposed surface area) and bioturbation, more extensively distributing the silicate amendment in the soil (Vicca et al., 2022). If silicates are redistributed to deeper soil layers, mineral dissolution may be enhanced due to greater soil CO_2 partial pressures (pCO_2) at depth (Winnick & Maher, 2018). Furthermore, earthworm burrows can increase water infiltration, decreasing the potential for saturation of soil pore water with reaction products that would limit further dissolution. A first chemical mechanism to enhance mineral dissolution is their placement in low pH environments. In this context, Liu et al. (2011) suggested enhanced dissolution through microbial activity in earthworm guts. Earthworm-enhanced dissolution of minerals is however unlikely to be driven by free (dissolved) protons as the

earthworm gut pH is typically around 6.5-7 (Carpenter et al., 2007). As a second potential chemical mechanism, an increase in respiration induced by earthworm activity would increase soil pCO_2 which may then increase mineral weathering (Lubbers et al., 2013). A third mechanism is the basic rule of chemical equilibrium, according to which a solution lower in a particular dissolved cation promotes dissolution of this cation from a solid. Earthworms can excrete solid carbonates from oesophageal (calciferous) glands (Darwin, 1981; Versteegh et al., 2014). As a base cation scavenger they may hence extract cations from the righthand side of reaction 1, shifting the equilibrium towards mineral dissolution, which may explain the potential chemical earthworm effect on weathering.

Earthworms have also been shown to produce clay minerals through soil ingestion and excretion (Carpenter et al., 2007; Hodson et al., 2014; Shipitalo & Protz, 1988). If these earthworm generated clays consume Ca^{2+}, Mg^{2+}, Na^{+} or K^{+} from soil water, soil water alkalinity and thus DIC are consumed. Base cations can be additionally scavenged from solution by exchange with OH groups on clays and organic molecules. Protons on OH-groups (abundant on clays) can deprotonate whereby O atoms scavenge base cations, stimulating the chemical equilibrium of reaction 1 towards mineral dissolution.

A larger exchange and precipitation of base cations with and in clays thus results in lower soil water alkalinity and DIC, while no carbonate precipitation occurs. Both base cation exchange and clay formation thus retard inorganic C sequestration. We expect that cations that are temporarily adsorbed in the exchangeable pool will be released and will become available to sequester inorganic C within climate mitigation relevant timeframes. Nonetheless, if the base cations precipitate within a clay mineral, this alkalinity is likely locked for longer than decadal timeframes as clays have low weathering rates; at neutral pH and 25°C for example, the base cation containing clays montmorillonite and smectite have a logarithmic weathering rate of -14.41 and -12.78 respectively. This is below the baseline log Wr of -

12.5, which was proposed by Bullock et al. (2022) to evaluate whether dissolution of a rock within decadal timescales is possible.

An increase in base cation exchange may however benefit soil C accumulation since base cations are known to stabilize soil organic carbon. It has been widely established that exchangeable Ca positively correlates with SOC (Rowley et al., 2018). Increased clay formation can furthermore stabilize organic matter via organo-mineral association, which is reflected in a typically positive correlation between SOC and soil clay content (Wiesmeier et al., 2019).

The relative contribution of chemical and physical mechanisms of earthworms to weathering can be explored using Si isotopes. Si has three stable isotopes: ^{28}Si (the most abundant isotope, at ca. 92.23%), ^{29}Si (ca. 4.67%), and ^{30}Si (ca. 3.09%). At steady-state, Si is released through weathering of silicates without any isotope discrimination (Ziegler et al., 2005). If however, silicon-bearing secondary phases (e.g. clays or amorphous silica) form, these typically discriminate against the heavier Si isotopes (Frings et al., 2014). Si isotopes thus show mineral dissolution indirectly: it is not the mineral dissolution itself, but the secondary clay formation that spurs on dissolution, that changes the isotope ratios. In addition, clay precipitation preferentially takes up Ge, decreasing the Ge/Si ratio in soil water. Hence, silicon isotope ratios (expressed as $\delta^{30}Si$, the deviation of the $^{30}Si/^{28}Si$ ratio from the NBS28 quartz standard) of dissolved Si resulting from the weathering process are generally elevated relative to the source minerals, with the magnitude of elevation of the $\delta^{30}Si$ value depending on the ratio of primary phase dissolution to secondary phase precipitation (Frings et al., 2021). We can conceptualise that if earthworms have no effect on the $\delta^{30}Si$ of dissolved Si that passed through the soil, any earthworm effect on (enhanced) weathering most likely involves only passive physical processes (e.g. burrowing effects). Conversely, if $\delta^{30}Si$ and Ge/Si change in soil water in the presence of earthworms, this indicates they actively influence the

(bio)geochemical weathering mechanisms. Silicon isotopes are thus a novel tool with which to probe the dynamics of biotically mediated enhanced weathering.

Earthworms cannot only impact inorganic carbon sequestration through EW, but can also impact the effect of silicate addition on soil organic carbon (SOC) sequestration. Earthworms can increase SOC stocks due to incorporation of plant litter into soils, and by forming stable soil aggregates. Soil aggregation is known to physically protect and stabilize SOC, and is influenced by mineral weathering as secondary minerals such as clay minerals and Fe- and Al-oxy-hydroxides which have a high SOC stabilization capacity by formation of a mineral associated organic matter (MAOM) fraction (<53µm) (Doetterl et al., 2018; Lavallee et al., 2020). Besides clay, Fe and Al, also Ca can protect SOC (Rowley et al., 2018). Minerals have been found to combine with SOC in earthworm casts, creating hotspots of MAOM (Vidal et al., 2019). Nevertheless, earthworm induced SOC stabilization mechanisms come with the cost of increased CO_2 emission through respiration of earthworms' associated microorganisms (Zhang et al., 2013). Predicting the direction, let alone the magnitude, of earthworm influence on SOC stocks in EW treatments is very challenging.

Questions also remain about how earthworms respond to EW treatments. The optimal pH for earthworms ranges between 6 and 8 (Jicong et al., 2005), and an EW-induced increase of soil pH in acid soils is thus expected to benefit earthworms (Desie et al., 2020). But, silicate weathering can also release heavy metals and elevated soil heavy metal contents have also been found to negatively affect earthworm abundance. For example, both Ni contents and mortality of *Aporectodea caliginosa* increased with increasing soil Ni content in ultramafic soils (Maleri et al., 2007; Maleri et al., 2008). We are unaware of further empirical evidence about the earthworm response to silicate amendments. Overall, little is known about the role of earthworms in soil inorganic and organic carbon sequestration during EW.

Here, we report results from a mesocosm experiment that evaluated (i) the impact of earthworms on basalt weathering and associated inorganic CDR, (ii) the impact of earthworms and basalt addition on SOC sequestration. (iii) cumulative soil CO_2 efflux (resulting from i and ii) within the experimental timeframe, and (iv) the impact of basalt addition on earthworm survival. This experiment furthermore allows us to investigate the fundamental dynamics of basalt enhanced weathering and to assess the competence of techniques for EW monitoring and CDR quantification.

2. Materials and Methods

2.1 Experimental set-up

An experiment with 28 mesocosms was set up and run for 137 days to investigate the effect of basalt addition (one treatment and control) and earthworms (two treatments and control) on C sequestration through EW. Mesocosms with dimensions 56×39×28 cm (area: 0.22 m²) were filled with 15 cm of soil delivered by the gardening center Vanderauwera (https://www.vanderauwera.be) (**Figure 1**; soil characteristics: See **Table 1**). Mesocosms were a box-in-a-box system, where the upper box was perforated to allow for leachate collection in the lower box (**Figure 1b**). The average temperature during this indoor experiment was 16±0°C. A total of six treatments was set up with or without anecic earthworms (*L. terrestris*), with or without endogeic earthworms (*A. caliginosa*), and with or without basalt, as summarized in **Table 2**. In the basalt treatments, 2.2 kg of Durubas basalt mesocosm^{-1} (equivalent to 100 t basalt ha^{-1}) was homogenously mixed into the soil using a concrete mixer. Endogeic earthworms were collected in a meadow at Campus Drie Eiken of Antwerp University and anecic earthworms were obtained from a commercial supplier (www.baitshop.nl). Five and four replicates per treatment were established for soils with and without basalt, respectively.

249 **Table 1: Characterization of control soil*.**

Control soil Characteristics	
Organic C (%)	0.97 ± 0.02
Texture (sand, silt, clay %)	silt loam (46.3, 51.4, 2.3)
Cation exchange capacity (CEC) (mEq/100g soil)	6.15 ± 0.21
Base saturation (%)	0.91 ± 0.02
Soil pH (in H_2O)	7.25 ± 0.04
Inoganic C (%)	0.32 ± 0.03
Basalt Characteristics (type: DURUBAS, RPBL)	
Mineralogical composition (from XRD)	(g/g)
Augite	0.50
Plagioclase	0.35
Olivine	0.05
Illite	0.05
Chlorite	0.05
BET Specific surface area	(9.226± 0.076) m^2/g
Particle size distribution	(mass %)
>2000µm	0.25 %
500-2000µm	0.52 %
250-500µm	22.30 %
63-250 µm	59.82 %
32-63 µm	14.73 %
<32 µm	2.38 %
XRF	(mass %)
SiO_2	44.6
MgO	12.9
CaO	10.8
K_2O	0.7
Na_2O	2.6
P_2O_5	0.9
Al_2O_3	11.5
Fe_2O_3	11.7
TiO_2	2.30

250 *Control soil was analyzed after the experimental period.
251 Values represent averages ± standard error of the mean.

(a) **(b)**

Figure 1: Mesocosm set-up: (a) top view of a mesocosm, with *Acer platanoides* leaves on the soil to feed earthworms and a central metal soil collar to measure CO_2 efflux. (b) Overview of the mesocosms' box-in-a-box system, where the upper box was perforated to allow for leachate collection in the lower box. In between sampling, lids were placed on mesocosms to prevent earthworm escape.

Table 2: Overview of experimental treatments. S= soil without earthworms and without basalt, SEA= soil with endogeic and anecic earthworms, without basalt. B= soil without earthworms but with basalt, BA = soil with basalt and anecic earthworms, BE= soil with basalt and endogeic earthworms, BEA = soil with basalt, endogeic and anecic earthworms.

Treatment code	S	SEA	B	BA	BE	BEA
Basalt (ton ha^{-1})	0	0	100	100	100	100
Number of endogeic earthworms	0	15	0	0	30	15
Number of anecic earthworms	0	15	0	30	0	15

At the start of the experiment (10 December 2021) mesocosms were watered until field capacity was reached for initial soil moisture equalization. After one week, 75 g of leaves (*Acer platanoides)* were added to each mesocosm as a food source for the earthworms. On the day before each leachate sampling, a total of 8 times, 1 L of tap water was added to every mesocosm. Tap water (pH 8.07 and TA 2.89 meQ L^{-1}) and basalt characteristics (50% augite, 35% plagioclase and 5% olivine) are provided in **Supplementary Tables 1 and Table 1**.

Water addition resulted in a percolation water flux (further referred to as leachate flux) equivalent to 130 mm $year^{-1}$. To allow for leachate collection, mesocosms had a 2 cm diameter hole at the bottom, which was covered with a root exclusion mat to prevent worm escape. Leachate water was collected in a glass recipient placed below the hole. Mesocosms were covered with a

lid in which small holes were drilled to allow for gas exchange. This also minimized water loss through evaporation. The last leachate sampling and gas measurements took place at 125 and 131 days after amendment, respectively. At 137 days after amendment (26th April 2021), soil was sampled for chemical analyses and for aggregate fractionation.

2.2 Leachate analyses

Leachate samples were filtered through a 0.45 µm PET syringe filter. Concentrations of Ca, Mg, K, Fe and Si were measured by ICP-OES (iCAP 6300 duo, Thermo Scientific). Na was only measured in the soil exchangeable pool and not in leachates. While we recognize the incompleteness of the base cation assessment, we expect that this omission does not affect our conclusions as for the other base cations the exchangeable fraction was at least 1 order of magnitude larger than leaching (**Table 6**). Before analysis, ICP samples were conserved using 1.5 mL (HNO_3 69%) per 30mL sample. pH was determined using a HI3220 pH/ORP meter. Total alkalinity (TA) and dissolved organic carbon (DOC) were determined colorimetrically using a Skalar (SAN++) continuous flow analyzer (SKALAR, 2022). TA was measured at each sampling occasion and dissolved inorganic carbon (DIC) was measured at one date in order to construct a DIC-TA calibration curve (**Supplementary Figure 1**). DIC was measured using a FormacsHT analyzer with LAS sampler (SKALAR).

2.3 Soil analyses

After 137 days of the experiment, soil cores (five cm in height and diameter) were taken for bulk density, cation exchange capacity (CEC) and C analyses. Immediately after collection, the cores were dried at 105°C for three days to determine dry soil bulk density (g m^{-3}), which was utilized to calculate soil dry weight per mesocosm. Dry soil weight was then used to upscale moles of exchanged cations per mass of soil to the total mass per mesocosm. Cation exchange capacity and exchangeable cations (Ca, Mg, Na, K) were measured with ICP-OES after extraction with 1 M ammonium acetate at pH 7 (Brown,

1943). Soil was sampled and subsequently divided into specific fractions by wet sieving as in Verbrigghe et al. (2022); dry soil was slaked for 5 min with DI water, after which it was wet-sieved through a 2 mm, 250 µm and 63 µm mesh. Each fraction was then dried at 70 °C for 72 h. In this way, the soil was separated into the following fractions: macroaggregates (>250 µm), sandy microaggregates (63 – 250 µm) and silt-clay microaggregates (<63 µm). Soil samples for C analysis were ground until smaller than 0.2 mm sieve with a ball mill (Mixer Mill MM200, Retsch GmbH, Haan, Germany), after which soil organic C (SOC) was removed in a muffle furnace (4 h at 360 °C, removing organic C but preventing loss of carbonates) (Dudhaiya et al., 2019). SOC was then calculated from the loss on ignition (LOI) assuming 58% C in soil organic matter (Van Bemmelen, 1890). Soil inorganic carbon (SIC) was quantified as the soil C remaining after LOI and was determined using an elemental analyzer (Flash 2000 CN Soil Analyser, Interscience, Louvain-la-Neuve, Belgium). After soil sampling, surviving earthworms were hand-sorted by type (endogeic/anecic) and counted.

2.4 Soil CO_2 efflux

Soil CO_2 efflux (SCE) was measured on 15 occasions (i.e., approximately weekly), using a cylindric chamber of known volume and area (0.98 L, 0.0082 m^2), which fitted on a collar that was permanently installed in the soil. The chamber was connected to a portable infrared CO_2 analyzer (EGM-5, PP systems, Hitchin UK). Each measurement lasted 120 seconds.

2.5 Si-isotope and Ge/Si analysis

Isotope ratio measurements of the silicon dissolved in the leachate waters collected from all mesocosms on day 6 and on day 82 were carried out at the Helmholtz Laboratory for Geochemistry of the Earth Surface (HELGES) at the German Research Centre for Geosciences GFZ. Silicon was separated from the cation matrix by ion exchange chromatography following the protocol outlined in Georg et al. (2006) in a class-100 laminar flow cabinet. Briefly, 1 ml of solution was directly loaded onto a column containing 1.5 ml

of AG 50W-X8 (200-400 mesh) cation exchange resin. A 100% Si yield was obtained through elution with milli-Q water after which ICP-OES analyses (Varian 720) determined the Si concentrations and confirmed the absence of any matrix elements. Prior to analysis, these Si solutions were diluted to 0.6 µg g^{-1} Si in a 0.1 M HCl matrix with 0.6 µg g^{-1} Mg. Silicon isotope ratios (expressed as $\delta^{30}Si$, the permil deviation in the $^{30}Si/^{28}Si$ ratio in the sample from the same ratio in the reference material NBS28 quartz sand) were determined with a Thermo-Fisher Neptune multi-collector inductively-coupled-plasma mass-spectrometer (MC-ICP-MS) operating in medium resolution ($m/\Delta m \approx 5000$). Sample solutions were thereby introduced to the plasma via an Apex-Q desolvation system and a self-aspirating nebuliser (flow rate ca. 120 µl min^{-1}). Instrumental mass-bias was corrected for by standard-sample bracketing with matrix-matched NBS28 solutions, using Mg isotope ratios measured in dynamic mode following (Cardinal et al., 2003).

Typical sensitivities after instrument tuning were about 15 V/ppm Si, resulting in a measurement signal of about 9V for our samples. Secondary reference materials measured in the same analytical session agree well with literature values (measured BHVO-2 $\delta^{30}Si \pm 1\sigma$ = -0.29±0.05‰, literature value = -0.28‰, (Savage et al., 2014); measured diatomite $\delta^{30}Si$ = 1.22±0.05‰, literature value = 1.26‰, (Reynolds et al., 2007)). The successful resolution of polyatomic interferences was demonstrated by all samples plotting on the expected mass-dependent fractionation line in a three-isotope plot. Long-term reproducibility in this laboratory is about ±0.15‰ (±2σ, (Oelze et al., 2016)), which we take as the uncertainty estimate unless internal precision was worse.

Following the recent demonstration that Ge elutes through the cation-exchange protocol together with Si (Delvigne et al., 2018; Frings et al., 2021), we also determined the Ge/Si ratio of leachate solutions. Ge/Si was analysed on the purified silicon solutions by quadrupole ICP-MS (qICP-MS) on a Thermo-Fisher iCAP-Q, using a collision cell (with He as a reaction gas at a

flow rate of 5 ml min^{-1}) to remove interferences on the Ge and Si isotopes. Calibration was relative to a series of gravimetrically prepared standards at constant Si but variable Ge. Full details are given in Frings et al. (2021). The Ge/Si ratio of the secondary standards BHVO-2 diatomite and nbs equalled 2.65, 0.64 and 0.36 µmol mol^{-1} respectively. In literature, BHVO-2 Ge/Si ranges from 2.45-2.70 µmol mol^{-1} (Frings et al. 2021). Quantification limits are <1 pg g^{-1}, equivalent to ca. 0.1 µmol mol^{-1} Ge/Si under the analytical conditions employed. Precision improves with increasing Ge content and is conservatively estimated to be about ±0.26 µmol mol Ge/Si (Frings et al. 2021). Accuracy was demonstrated by satisfactorily reproducing literature values (included those generated by the benchmark hydride generation and isotope dilution technique; (Mortlock & Froelich, 1996) for the secondary reference materials BIR-1a, BHVO-2, Diatomite and NBS28.

2.6 Data analyses

To calculate a cumulative SCE, the average treatment CO_2 flux was determined for each measurement and then interpolated linearly between two measurements in time. The cumulative mass of leached DIC was calculated by multiplying leachate volumes and DIC concentrations for each sampling date and summation over all sampling dates, after which the mass of cumulative DIC leaching was converted into ton CO_2 equivalents ha^{-1}. We then calculated TIC (total inorganic C) as the sum of SIC and DIC.

For SIC, SOC, CEC, cumulative SCE, base saturation and aggregate fractionation data, a multi-way ANOVA analysis with basalt addition and earthworm type (endogeic and anecic earthworms) as fixed factors was done in order to identify significant effects of basalt or earthworm species. Four levels of interactions (Basalt (0/1) and earthworm (0/1)) were tested in all statistical analyses. For measurements that were repeated in time (leachate compositions), a mixed linear model was used with basalt, anecic earthworms, endogeic earthworms and time as fixed factors and mesocosm

as a random factor using the lme4 package. Here, basalt × time interaction was also tested to investigate changes of the basalt effect in time. The assumption of normally distributed residuals was verified using a Shapiro-Wilk test. If residuals were not normally distributed after log10 data transformation a Generalised Additive Mixed Model (GAMM) was constructed using the mgcv R package. To investigate statistical differences between endogeic and anecic worm survival in basalt mesocosms, a pairwise Tukey comparison between treatment BA and BE was done. In order to assess the effect of basalt on worm survival, Tukey tests were performed comparing the SEA-BEA and BE-BA treatments. All analyses were executed in R studio (R-4.0.5).

2.7 Estimating inorganic CDR equivalents by cation charge balancing

Cation charge balancing can shed more light on inorganic CDR equivalents. As basalt weathers (Reaction 1), first alkalinity is transferred from primary minerals to soil water as HCO_3^- and base cations (e.g. Ca) increase in the soil solution. As already pointed out in the introduction, These base cations can be exported with soil water (=alkalinity leaching), form a pedogenic carbonate, precipitate as clays or exchange with protons. If base cations precipitate as clay minerals (e.g. montmorillonite or smectite), alkalinity is likely locked up for a long time, retarding inorganic CDR beyond timescales relevant for current climate change.

In a more optimistic scenario for inorganic CDR, exchange with protons on ROH-groups occurs (with R being Si if the exchanging molecule is a clay, or R being a C atom if the exchanging molecule is an organic compound). If a base cation such as Ca exchanges with 2 ROH-groups, 2 RO-Ca bounds are formed and 2 protons are released in solution, neutralizing HCO_3^- that was formed in Reaction 1 to H_2CO_3. As H_2CO_3 is in equilibrium with H_2O and

CO_2, this leads to degassing of inorganic C to CO_2 and alkalinity is transferred to the exchangeable pool.

During the temporary alkalinity storage in the exchangeable pool, base cations can exchange with organic acids (e.g. in an CO-Ca-OC bound), whereafter organic C adsorbs to the soil and may not become available as DOC for microbial respiration. We do not expect the latter SOC stabilization if the exchanged cations form SiO-Ca-OSi bounds as in this case, the base cation exchange does not adsorb DOC. An increase in exchanged cations thus has the potential to increase SOC stabilization, but this is not necessarily the case. As the capacity of a soil to hold cations in adsorbed sites is finite, after a transient period cations will be released from the exchangeable pool and leach out, releasing alkalinity back in the soil solution, causing DIC to increase.

As inorganic CDR does not happen as long as base cations are retarded in the exchangeable pool, we used the charge balance to convert dissolved base cations into 'Inorganic CDR equivalents'. 'Inorganic CDR equivalents' is a more conservative approach for CDR calculation than the approach where all generated alkalinity was considered as CDR (as e.g. used in Kantola et al., 2023). The latter does not take into account potential HCO_3^- degassing with protons in the time until generated alkalinity reaches the ocean. Moreover, we opt to only use the terminology 'CDR' when we actually measured reductions in SCE. The latter includes not only inorganic C fluxes, but also organic C fluxes.

In literature, the term CDR potential (or enhanced weathering potential (Epot)) is used to predict the maximum CO_2 sequestration potential of unweathered rocks based on their Na_2O, K_2O, CaO and MgO content (Renforth et al., 2019). We propose to explicity call this a 'theoretical

inorganic CDR potential' and distinguish this from 'inorganic CDR equivalents' which need to be experimentally verified after a certain period of rock weathering.

In order to estimate the inorganic CDR equivalents here, minimal dissolution rates per treatment are calculated from the sum of excess exported leachate cations and the increase in exchangeable base cations in a treatment (E.g. treatment 'B') relative to the control treatment 'S'. This is a minimal weathering rate and hence minimal inorganic CDR equivalent rate as dissolved cations could also go to reducible and oxidizable soil pools which were not assessed here and have not been assessed in EW experiments to the best of our knowledge (Tessier, Campbell, & Bisson, 1979).

If we consider TA as the sum of conservative cations (2*(Ca + Mg) + Na + K)) as in Barker et al. (2013) and Wolf-Gladrow et al. (2007) and assume conservative anions (such as Cl^- and SO_4^{2-}) not to change among treatments, we can convert moles of base cations into moles of alkalinity. Using the specific surface area of the utilized basalt (**Table 1**), the minimal weathering rate (mWr) per surface area of basalt (in mol base cation m^{-2} basalt s^{-1}) was calculated. This was done for alkalinity as a whole (**Equation 1)** and for each element separately **(Equation 2)**. Note that leachate Na is not included in equation 1. We think that neglecting Na in leachates would not lead to major changes in the outcome of results as cations in the exchangeable pool were always 1 order of magnitude larger than leachate cations in this experiment.

$$\text{Log Wr,j}\left[\frac{\text{molTA}}{m^2.s}\right] = \text{Log}_{10}\left(\frac{\sum_{i=1}^{n}(\Delta K_{i,j} + 2\Delta Ca_{i,j} + 2\Delta Mg_{i,j}) + (\Delta K_{exch,j} + \Delta Na_{exch,j} + 2\Delta Mg_{exch,j} + 2\Delta Ca_{exch,j})\left[\frac{\text{mol TA}}{\text{mesocosm}}\right]}{Basalt\ application\ rate\left[\frac{g\ Basalt}{mesocosm}\right] * (BET - SSA)\left[\frac{m^2 Basalt}{g\ basalt}\right] * Experimental\ duration\ [s]}\right) \quad \textbf{Eq.1}$$

$$\text{Log Wr,j}\left[\frac{\text{mol element}}{m^2.s}\right] = \text{Log}_{10}\left(\frac{\sum_{i=1}^{n}(\text{element charge} * (\Delta\text{element}_{i,j} + \Delta\text{element}_{exch,j})\left[\frac{\text{mol element}}{\text{mesocosm}}\right])}{Basalt\ application\ rate\left[\frac{g\ Basalt}{mesocosm}\right] * (BET - SSA)\left[\frac{m^2 Basalt}{g\ basalt}\right] * Experimental\ duration\ [s]}\right) \quad \textbf{Eq.2}$$

With Basalt application rate = 2200 g mesocosm^{-1}, BET-SSA basalt = 9.226 m^2 g^{-1} and experimental duration = 137 days or 11836800 seconds. For a certain treatment j relative to treatment 'S' (With n = number of leachate sampling dates). Δelement_i,j, ΔK_i,j, ΔCa_i,j ,ΔMg_i,j the thus represent the delta of leached moles per mescosom between treatment j and 'S' for a certain date i. Δelement_exch,j, ΔK_exch,j, ΔMg_exch,j and ΔCa_exch,j represent the relative difference (treatment j – treatment S) in moles of exchanged base cations in soils sampled after 137 days of experiment.

Using a conversion factor of 1 mole of HCO_3^- per mole of cation charge equivalent (in other words 1 mol CO_2/mol TA, maintaining the charge balance of Reaction 1; see also Dietzen et al. (2018) and ten Berge et al. (2012)) cations that were dissolved from primary minerals are subsequently converted into inorganic CDR equivalents (**Equation 3)**. This assumes that all dissolved cation charge generates a mol of bicarbonate (for monovalent cations we conceptualize a factor η^+ = 1 mol CO_2/mol cation and for divalent cations a factor η^{++} = 2 mol CO_2/mol cation).

We can generalize **Equation 3** (where η^{++} = 2 and η^+ = 1) as **Equation 4**.

$$\text{Inorganic CDR equivalents}\left[\frac{\text{molCO2}}{mesocosm}\right] = \frac{2 * \text{mol cation}^{++}\text{ dissolved} + 1 * \text{mol cation}^{+}\text{ dissolved}}{mesocosm} \quad \textbf{Eq. 3}$$

$$\text{Inorganic CDR equivalents}\left[\frac{\text{molCO2}}{mesocosm}\right] = \frac{(\eta^{++} * \text{mol cation}^{++}\text{ dissolved}) + \eta^{+} * \text{mol cation}^{+}\text{dissolved}}{mesocosm} \quad \textbf{Eq. 4}$$

Renforth et al. (2019) conceptualized the "enhanced weathering" potential (E_{pot}) of a rock, assuming that all dissolved cations (reaction 1) reach the

ocean without carbonate degassing (reaction 2). Still, after equilibrium in the ocean system, a portion of DIC degasses so that in reality, if DIC reaches the ocean, the factor η^{++} is reduced to $[1.4, 1.72]$ and η^{+} to $[0.7, 0.86]$ (Bertagni & Porporato, 2022; Renforth, 2019). Renforth et al. (2019) also defined a more conservative scenario where all divalent cations form a solid carbonate according to Reaction 2: mineral carbonation (resulting in η^{++} =1). These carbonates can either precipitate in soils or, as recently modelled by Knapp & Tipper (2022), even if DIC is exported from soils, solid carbonates can form in rivers oversaturated in carbonates. In agreement with Renforth et al. (2019), we do not consider degassing through carbonate formation from monovalent cations since, to the best of our knowledge, pedogenic formation of Na or K carbonates does not occur.

In **Table 6**, we calculate inorganic CDR equivalents (prior to ion leaching to the ocean, hence η^{++} =2 and η^{+} =1 or in other words 1 mol CO_2 mol^{-1} TA) from the weathering rate as in Amann et al. (2022). In addition, in a more pessimistic scenario of η^{++} =1 (carbonate degassing scenario), all divalent cations form pedogenic carbonates (**Table 6**). The units of these inorganic CDR equivalents were converted from mol $mesocosm^{-1}$ to ton CO_2 ha^{-1} (**Equation 5**).

$$\text{Inorganic CDR equivalents}[\text{ton CO2 ha} - 1] = \frac{\text{Inorganic CDR equivalents}[\frac{\text{mol CO2}}{mesocosm}]}{area\,[\frac{m^2}{mesocosm}]} * \frac{10000\text{m}^2}{ha} * 44\,\frac{\text{gCO2}}{mol\ CO2} * \frac{1\ tonCO2}{10^6 g\ CO2} \quad \textbf{Eq. 5}$$

We can also express this in ton CO_2 ton $basalt^{-1}$ $year^{-1}$ by dividing with the basalt application rate (in ton ha^{-1}) and the experimental duration in years.

3. Results

3.1 Inorganic CDR

Basalt addition clearly increased leachate DIC (**Figure 2a**), although this effect is quantitatively modest: only approximately 40 kg CO_2 ha^{-1} $year^{-1}$ was sequestered through DIC (**Figure 3)**. Earthworms slightly reduced leachate

DIC (**Figure 2a, Table 3**). No significant effects of basalt or earthworms on SIC could be detected after 137 days (**Figure 2b, Table 3**).

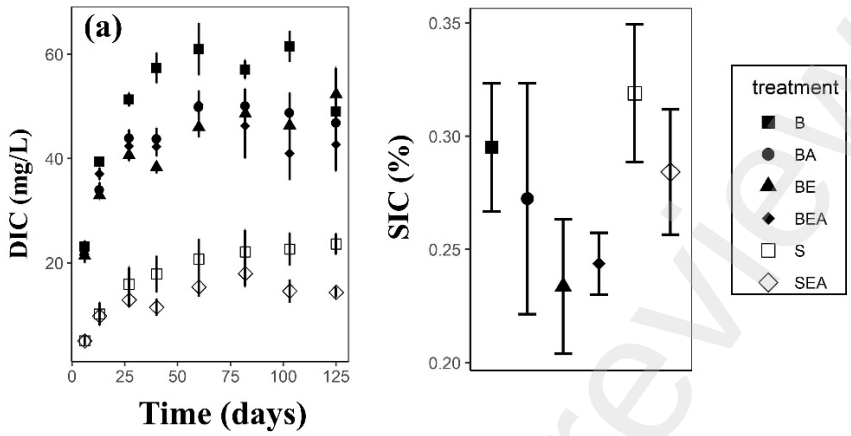

Figure 2: (a) Leachate DIC as a function of time. (**b)** SIC among treatments after 137 days. Error bars represent standard errors on the average.

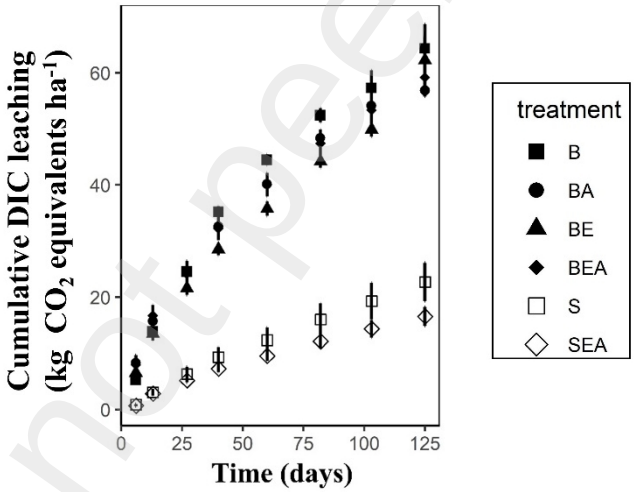

Figure 3: Cumulative DIC leaching as a function of time. Error bars represent standard errors on the average.

3.2 Effects on organic carbon

Basalt addition significantly increased DOC leaching and earthworms, similar to DIC, significantly decreased leachate DOC (**Figure 4a, Table 3**). Neither basalt nor earthworms addition induced significant changes in SOC concentration or soil aggregate formation (**Figure 4b and 5, Table 3).** No significant interaction effects between basalt addition and earthworms presence were found.

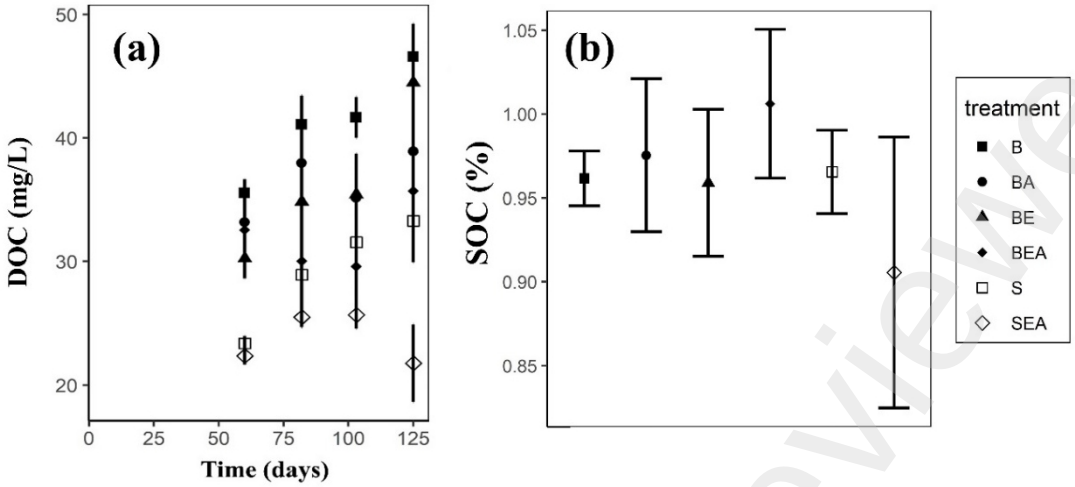

559 **Figure 4: (a)** Leachate DOC as a function of time and **(b)** SOC at the end of
560 the experiment. Error bars represent standard errors on the average.

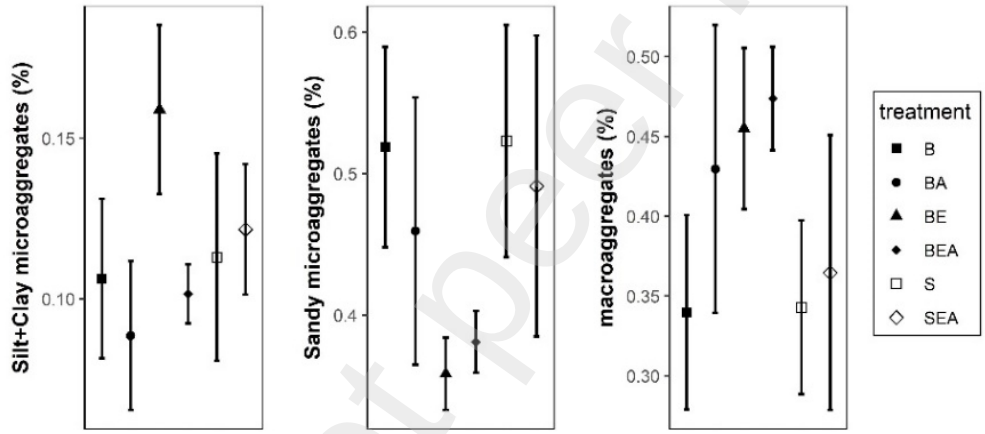

561 **Figure 5:** Effects of basalt, anecic and endogeic earthworms on aggregate
562 mass fractions in the soil. Error bars represent standard errors on the average.

563 **Table 3:** Effects of basalt, anecic earthworms and endogeic earthworms and
564 the combination of basalt and worms on soil carbon (DIC, DOC, SIC, SOC)
565 and aggregate fractions. Values represent averages ± standard error of the
566 mean. A '+' indicates a significant increase ($p<0.05$), while '-' reflects a
567 significant decrease. N.S. = Not Significant indicates that interaction terms
568 were not statistically significant. Non-significant effects are indicated in
569 italics, while significant effects are indicated in bold.

Parameter	**Basalt** (effect)	**Endogeic** (effect)	**Anecic** (effect)	**Worm x Basalt** (effect)
DIC (mg L^{-1})	p<0.01**(+28.41)**	p<0.01**(-4.28)**	p<0.01**(-2.78)**	N.S.
DOC (mg L^{-1})	p<0.01 **(+9.88)**	p<0.01 **(-3.81)**	p<0.01 **(-3.75)**	N.S.
SIC (%)	p=0.25 *(-0.04)*	p=0.14 *(-0.04)*	p=0.91 *(-0.00)*	N.S.
SOC (%)	p=0.45 *(+0.03)*	p=0.87 *(-0.01)*	p=0.76 *(+0.01)*	N.S.
Macroaggregates (%)	p=0.21 *(+7.32)*	p=0.35 *(+5.20)*	p=0.63 *(+2.67)*	N.S.
Sandy microaggregates (%)	p=0.21 *(-8.01)*	p=0.13 *(-9.30)*	p=0.89 *(+0.79)*	N.S.
Silt/clay microaggregates (%)	p=0.88 *(-0.31)*	p=0.08 *(+3.54)*	p=0.08 *(-0.31)*	N.S.

570

3.3 Soil CO_2 efflux

Compared to the control, basalt significantly decreased SCE (**Table 4**). By the end of the experiment, after 131 days, 1.96±0.62 ton CO_2 ha^{-1} efflux reduction was observed in the non-worm basalt ('B') treatment relative to the non-worm control soil (treatment 'S') (**Figure 6b).** However we do not observe a reduction in CO_2 emissions if besides basalt, also earthworms were added to soils. Comparing treatments BA, BE and BEA with the unamended control soil treatment S, we observe an average increase in SCE of 1.25, 1.64 and 2.00 ton CO_2 ha^{-1} respectively (**Table 6**). Also in non-basalt soils, we observe an increase in SCE after earthworm addition. However, the increase in SCE due to addition of earthworms was larger in basalt relative to non-basalt soils (**Figure 6b**).

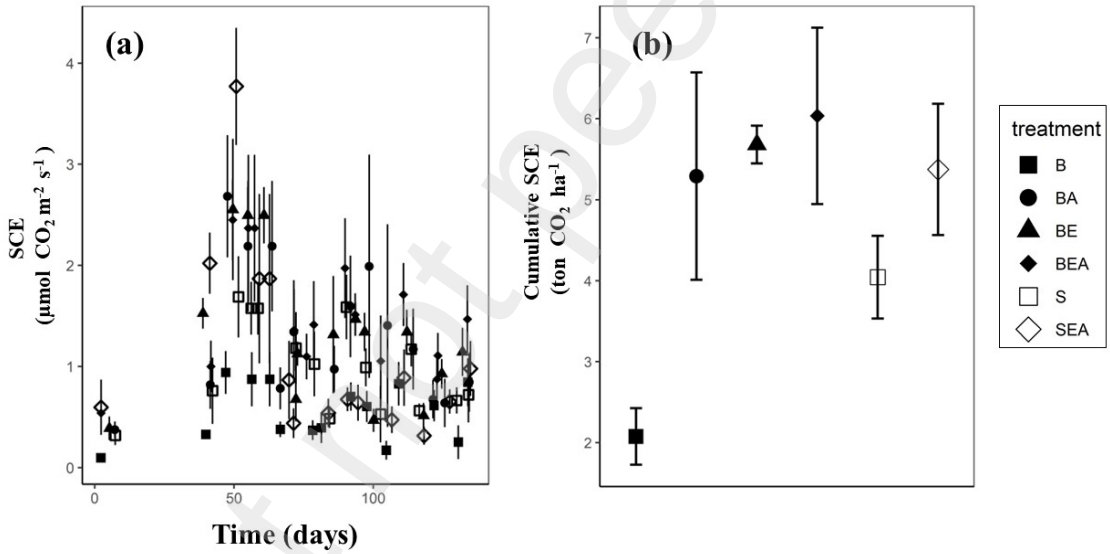

Figure 6: (a) soil CO_2 efflux (SCE) as a function of time after amendment and (b) cumulative SCE 131 days post amendment. Error bars represent standard errors on the average.

3.4 Products of mineral dissolution in leachates and the soil exchangeable pool

3.4.1 Mineral dissolution products in leachates

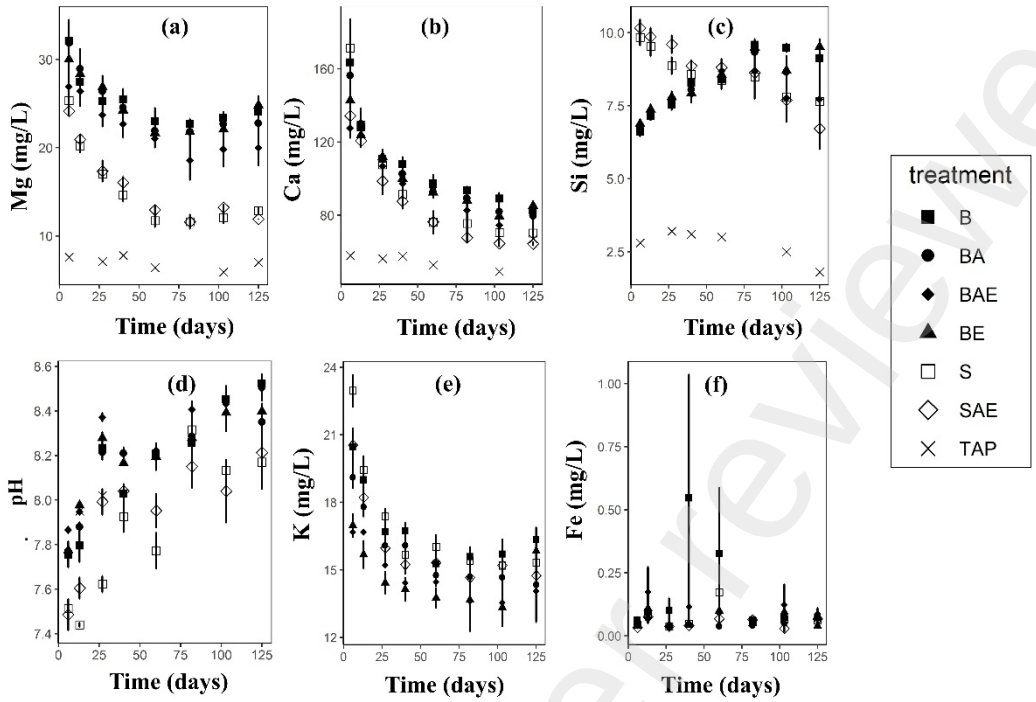

Figure 7: Leachate concentrations of (a) Mg (b) Ca (c) Si and (d) pH (e) K and (f) Fe as a function of time. Basalt treatments are indicated in bold. TAP represents concentrations in input tap water. Error bars represent standard errors on the average.

Across all treatments, we observed an initial pulse in leaching of Mg and Ca that gradually decreased over the course of the experiment. Addition of basalt led to an increase of leachate pH, Mg, Ca and TA; a positive effect that somewhat increased over time (**Figure 7 and 8**). The effect of basalt on dissolved Si and K in leachate switched from an initial decrease (negative) to an increase (positive) over the course of the experiment (**Table 4**).

Both anecic and endogeic earthworms significantly decreased leachate TA and Ca (**Figure 7 and 8, Table 4**). Earthworms decreased leachate TA, Si, K more in the presence of basalt. Endogeic worms increased Mg leaching without basalt, yet in the presence of basalt, endogeic earthworms also caused a decrease in Mg leaching. In general, the negative earthworm effects on the abovementioned leachate parameters are small compared to the basalt-induced increases (**Figure 7 and 8)**.

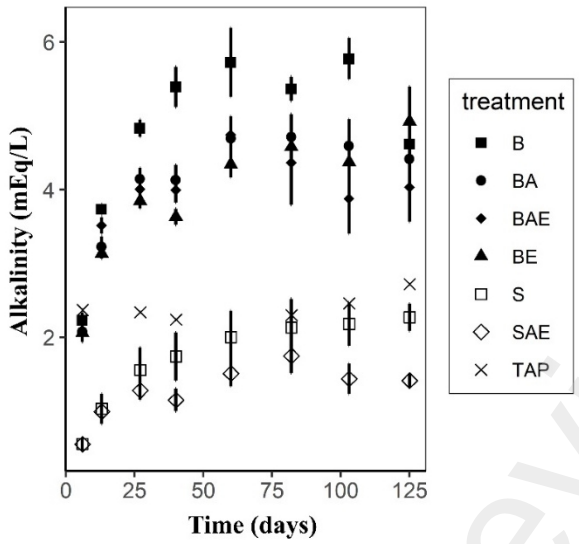

Figure 8: Leachate TA as a function of time. TAP represents the input tap water alkalinity. Error bars represent standard errors on the average.

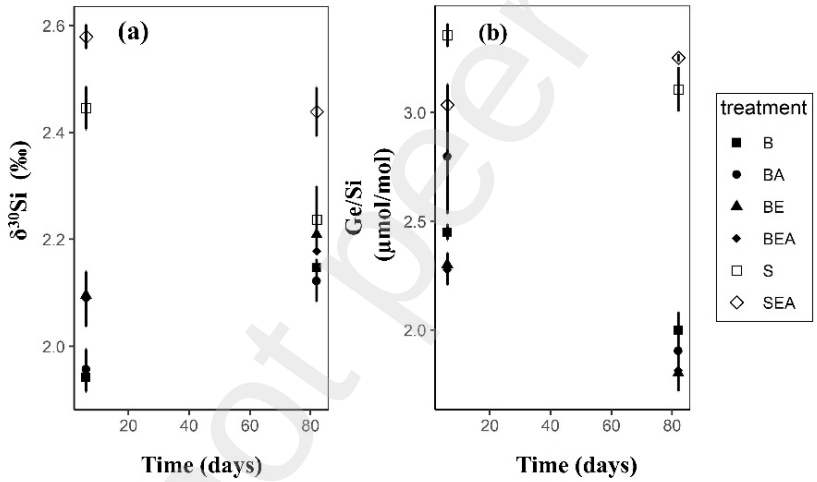

Figure 9: (a) Silicon isotope ratios ($\delta^{30}Si$) and (b) Ge/Si ratios in leachate samples as a function of time. Error bars represent standard errors on the average.

Basalt amendment reduced $\delta^{30}Si$ and Ge/Si in the leachates (**Figure 9, Table 4**). However, whereas this basalt effect on $\delta^{30}Si$ decreased over time, the basalt effect on the Ge/Si ratio increased over time. A positive and negative endogeic worm effect was observed on leachate $\delta^{30}Si$ and Ge/Si, respectively, while there was no significant basalt x earthworm interaction effects for $\delta^{30}Si$ or Ge/Si (**Table 4**).

Table 4: Effects of basalt, anecic and endogeic earthworms on parameters that were repeatedly measured in time (leachate concentrations and cumulative SCE). Values represent averages ± standard error of the mean. '+' indicates a significant increase ($p<0.05$), while '-' reflects a significant decrease. N.S. = Not Significant indicates that interaction terms were not statistically significant. Non-significant effects are indicated in italics, while significant effects are indicated in bold.

Parameter (unit)	**Basalt effect** (unit)	**Endogeic effect** (unit)	**Anecic Effect** (unit)	**Basalt × Time** (unit /day)	**Basalt × Earthworm** (unit)
Mg (mg/L)	p<0.01 **+8.52**	p=0.04 **+1.78**	p<0.01 **-1.45**	p<0.01 **+0.03**	p<0.01 **-3.37**
Ca (mg/L)	p=0.58 *+1.76*	p=0.03 **-6.40**	p<0.01 **-3.88**	p<0.01 **+0.14**	N.S.
Si (mg/L)	p<0.01 **-2.50**	p=0.05 *+0.46*	p=0.02 **-0.30**	p<0.01 **+0.04**	p=0.02 **-0.61**
pH (-)	p<0.01 **+0.02**	p=0.10 *+0.05*	P=0.23 *+0.04*	p<0.01 **+0.01**	N.S.
TA (mEq/L)	p<0.01 **+2.32**	p<0.01 **-0.40**	p<0.01 **-0.26**	p=0.02 **+0.01**	N.S.
K (mg/L)	p<0.01 **-1.46**	p=0.23 *-0.47*	p=0.03 **-0.46**	p<0.01 **+0.02**	p<0.01 **-1.21**
Fe (mg/L)	p=0.26 *+0.03*	P=0.50 *-0.02*	P=0.24 *-0.03*	N.S.	N.S.
δ^{30}Si (‰)	**p<0.01 -0.42**	**p<0.01 +0.12**	p=0.73 *0.01*	p<0.01 **+0.00**	N.S.
Ge/Si (µmol/mol)	p<0.01 **-0.68**	p<0.01 **-0.22**	p=0.25 *+0.08*	p<0.01 **-0.01**	N.S.
Cumulative SCE after 131 days (ton CO_2 ha^{-1})	p<0.01 **-0.76**	p=0.11 *+0.45*	p<0.01 **+0.95**	N.S.	p<0.01 **+1.01**

3.4.2 Mineral dissolution products in the exchangeable pool

Dissolved ions can (albeit temporally) be retained by cation exchange in soils. Relative changes among treatments after 137 days of mineral dissolution are shown in **Table 5**. Basalt increased exchangeable Ca, Mg, Na and K in soil. In addition, Ca, Mg and K exchange was stimulated by the combination of basalt with earthworms (**Table 5**).

Table 5: Cation exchange capacity (CEC), base saturation and contribution of exchanged elements of soils sampled 137 days after soil amendment. Values represent averages ± standard error of the mean. A '+' indicates a significant increase ($p<0.05$), while '-' reflects a significant decrease. N.S. = Not Significant indicates that interaction terms were not statistically significant. Non-significant effects are indicated in italics, while significant effects are indicated in bold.

Treatment	CEC (mEq/100g)	Na	K	Ca	Mg	H^+	Al	Fe	Mn	Base saturation (%)
B	7.08 ± 0.11	0.21±0.02	0.39±0.01	5.34±0.10	1.01±0.02	0.09±0.05	0.014± 0.001	0.004± 0.000	0.011± 0.004	0.98± 0.01
BA	6.96 ± 0.06	0.22±0.02	0.40±0.01	5.17±0.09	1.07±0.01	0.07±0.04	0.014± 0.001	0.003± 0.000	0.008± 0.002	0.99± 0.01
BE	7.25 ± 0.12	0.20±0.01	0.39± 0.01	5.51±0.13	1.08±0.02	0.03±0.02	0.013± 0.000	0.007± 0.001	0.016± 0.003	0.99± 0.00
BEA	7.97 ± 0.30	0.22±0.01	0.43±0.01	6.16±0.32	1.12±0.04	0.02±0.02	0.015± 0.001	0.005± 0.001	0.010± 0.003	0.99± 0.00
S	6.15 ± 0.21	0.08±0.01	0.31±0.00	4.54±0.29	0.65±0.02	0.53±0.12	0.014± 0.000	0.007± 0.000	0.021± 0.005	0.91± 0.02
SEA	5.95 ± 0.11	0.06±0.01	0.30± 0.00	4.26± 0.15	0.65±0.01	0.64±0.06	0.014± 0.000	0.005± 0.000	0.011± 0.001	0.89± 0.01
Basalt effect	p<0.01 **+0.74**	p<0.01 **+0.14**	p<0.01 **+0.08**	p=0.03 **+0.61**	p<0.01 **+0.36**	p<0.01 **-0.53**	p=0.90 *+0.000*	p<0.01 **-0.002**	p=0.15 *-0.004*	p<0.01 **+0.09**
Anecic effect	p=0.13 *+0.27*	p=0.06 *+0.01*	p=0.04 **+0.02**	p=0.28 *+0.21*	**p=0.02** **+0.05**	p=0.61 *+0.02*	p=0.34 *+0.000*	**p=0.01** **-0.001**	**p=0.03** **-0.007**	p=0.66 *-0.00*
Endogeic effect	p=0.16 *-0.47*	p=0.02 **-0.01**	p=0.08 *-0.02*	p=0.18 *-0.49*	p=0.19 *-0.05*	p=0.75 *-0.02*	p=0.94 *+0.000*	p=0.88 *-0.000*	p=0.73 *+0.001*	p=0.90 *+0.00*
Basalt x Earthworm effect	p=0.01 **+1.04**	N.S.	p=0.02 **+0.04**	p=0.02 **+1.04**	p=0.02 **+0.11**	N.S.	N.S.	p=0.02 **+0.002**	N.S.	N.S.

3.5 Determination of weathering rates and inorganic CDR equivalents

Based on leachate and cation exchange data (**Table 4 and 5**), the 'minimal weathering rate (mWr)' and inorganic CDR equivalents are calculated in Table 6. (explanation of these terms, see section 2.7). We observe that basalt increased the mWr and inorganic CDR equivalents in treatment 'B', the basalt treatment without earthworms (**Table 6**). We also observed a reduction in SCE relative to the control in this treatment (**Figure 6b).** This reduction of SCE is larger than the calculated inorganic CDR equivalents.

Nonetheless, larger inorganic CDR equivalents did not always correspond with a lower SCE; we observed increases of soil CO_2 emissions in basalt treatments with earthworms relative to the control, while in these treatments earthworms stimulated mWr and increased inorganic CDR equivalents.

Table 6: Minimal dissolution rates of Ca, Mg, Na and K through changes in base cation exchange and leaching relative to the control non-worm soil (treatment 'S') after 137 days of weathering and TA dissolution rate calculated from these four base cations. Equivalent moles of CO_2 that reacted during dissolution of divalent cations are calculated for two endmember scenarios: (1) $\eta^{++} = 2$ (1 mol CO_2/ mol charge dissolved) and (2) $\eta^{++} = 1$. For monovalent cations, η^{+} is set equal to 1 in all scenarios (Equation 3 and 4). Log minimal weathering rates (Log mWr) are marked in gray and scales with inorganic CDR equivalents. The effect on the delta soil CO_2 efflux (ΔSCE) is also shown for comparison. All values represent means ± the standard error on the mean. Underlying data on cation leaching and exchange can be consulted in Table 4 and 5. Calculation of these data is described in section 2.7.

Parameter	**unit**	Treatment				
Expressed as the difference between the treatment and control non-worm soil (treatment S)		B	BA	BE	BEA	SEA
Δcumulatively Leached cations (underlying data: Table 3)	mmol Ca/column	1 ± 2	3 ± 2	6 ± 3	3 ± 3	0 ± 2
	mmol Mg/column	3 ± 1	4 ± 1	5 ± 1	4 ±1	1 ±1
	mmol K/ column	0 ± 0	0 ± 0	0 ±0	0 ±0	0 ±0
	mmol Na/ column			Not determined		
ΔExchanged cations (underlying data: Table 4)	mmol Ca/ column	163 ± 54	116 ± 53	226 ± 53	302 ± 71	-24 ±56
	mmol Mg/ column	66 ± 7	71 ± 6	84 ± 6	85 ± 8	3 ± 5
	mmol K/ column	32 ± 5	30 ± 5	37 ± 5	43 ± 5	1 ± 4
	mmol Na/ column	45 ± 3	49 ± 4	44 ± 2	48 ± 3	-5 ± 2
ΔLeached + Δexchanged cations (total)	mmol Ca/ column	164 ± 54	119 ± 53	233 ± 54	304 ± 71	-24 ± 56
	mmol Mg/ column	69 ± 7	76 ± 6	89 ± 6	88 ± 8	4± 5
	mmol K/ column	32 ±5	30 ± 5	37 ± 5	43 ± 5	0 ± 4
	mmol Na/ column	45± 3	49 ± 4	44 ± 2	48 ± 3	-5 ± 2
Minimal Weathering rate (mWr)	10^{-14} mol Ca/m² basalt/s	68 ± 23	50 ± 22	97 ± 22	127 ± 29	-10 ± 23
	10^{-14} mol Mg/m² basalt/s	29 ± 3	32 ± 2	37 ± 2	37 ± 3	2 ± 2
	10^{-14} mol K/m² basalt/s	13 ± 2	12 ± 2	16 ± 2	18 ± 2	0 ±2
	10^{-14} mol Na/m² basalt/s	23 ± 1	20 ±2	18 ± 1	20 ± 1	-2 ±1
	10^{-14} Mol TA/m² basalt/s	226 ± 46	195 ± 44	302 ± 45	365 ± 59	-18 ± 47
Log minimal weathering rate Log (mWr)	**Log TA/m²/s**	**-11.65± 0.09**	**-11.71± 0.10**	**-11.52± 0.06**	**-11.44± 0.07**	**mWr<0, no log**
Inorganic CDR equivalents: HCO_3^- export scenario $\eta^{++} = 2$, $\eta^{+} = 1$ (=1 mol CO_2 mol^{-1} TA)	Ton CO_2 ha^{-1}	1.09 ± 0.22	0.94 ± 0.21	1.45 ± 0.22	1.75 ± 0.28	-0.09 ± 0.22
	Ton CO_2 ton $basalt^{-1}$ $year^{-1}$	0.029± 0.006	0.025± 0.006	0.039± 0.006	0.047± 0.008	-0.002± 0.006
Inorganic CDR equivalents: solid carbonate scenario $\eta^{++} = 1$, $\eta^{+} = 1$	Ton CO_2 ha^{-1}	0.62±0.11	0.55± 0.11	0.81±0.11	0.97±0.14	- 0.05±0.11
	Ton CO_2 ton $basalt^{-1}$ $year^{-1}$	0.017 ± 0.003	0.015 ± 0.003	0.021 ± 0.003	0.026 ± 0.004	-0.001± 0.003
Soil CO_2 efflux (ΔSCE) reduction (This is CDR if values are positive)	Ton CO_2 ha-1	1.96± 0.62	-1.25 ± 1.38	-1.64 ± 0.56	-2.00 ± 1.20	-1.33 ± 0.96
Soil CO_2 efflux (ΔSCE) reduction (This is CDR if values are positive)	Ton CO_2 ton $basalt^{-1}$ $year^{-1}$	0.055 ± 0.017	-0.035 ± 0.038	-0.046 ± 0.016	-0.056 ± 0.034	-0.035± 0.026

3.6 Earthworm survival

On average, survival rates of endogeic earthworms were between 52-70% and survival rates of anecics between 52-63% (**Table 7**). We did not observe significant differences in survival rate of endogeic (p=0.95) and anecic earthworms (p=0.96) after comparison of treatments BEA and SEA. When comparing treatments BE and BA, earthworm survival rates were higher for endogeic than for anecic earthworms (p=0.04).

Table 7: Earthworm survival rates after 137 days of experiment (average±se). Non-significant effects are indicated in italics, while significant effects are indicated in bold.

Treatment	Initial # of endogeic worms	Initial # of anecic worms	Final # of anecic worms	final # of endogeic worms	Survival rate endogeic worms (%)	Survival rate anecic worms (%)	Pairwise comparison earthworm survival	Pairwise comparison anecic survival	Pairwise comparison endogeic survival
BE	/	30	/	21±2	70±6	/	**BE-BA= 5** (p=0.04)		
BA	30	/	16±1	/	/	52±4			
SEA	15	15	9±2	9±2	62±13	63±10		*SEA-BEA=2* (p=0.96)	*SEA-BEA=2* (p=0.95)
BEA	15	15	8±3	8±1	52±4	52±19			

4. Discussion

4.1 Basalt

4.1.1 Basalt weathering and inorganic CDR

As silicates weather, Si is dissolved and can precipitate as SiO_2 and clays. Changes in soil water Si can thus provide insights into (basalt) weathering processes. In our experiment, Si was initially the only element in the leachates that was lower in the basalt treatments than in the treatments without basalt (**Figure 7**). This does not imply that Si was not dissolved from silicate minerals at the onset of the experiment, as other elements (Ca and Mg) increased in the leachates. We infer that initially, the Si precipitation rate was larger than Si release by weathering, causing Si concentration in leachates to decrease. This Si bearing precipitate could be a clay such as kaolinite (or another allophane-like phase), or amorphous SiO_2.

The possibility of Si bearing secondary phase formation argues against usage of dissolved Si concentrations as a tracer for EW as was done in the recent

work of Wood et al. (2022). Here, we use soil water $\delta^{30}Si$ and Ge/Si rather than just Si concentrations as a novel alternative for EW monitoring. Clay precipitation preferentially takes up lighter Si and Ge, decreasing $\delta^{30}Si$ and Ge/Si in soil water. Early on in the experiment, $\delta^{30}Si$ and Ge/Si were indeed lower in basalt treatments than in the non-basalt treatments (**Figure 9**) which suggest the formation of clay minerals. Over time however, the $\delta^{30}Si$ in the leachates of the basalt treatment increased, suggesting a reduction in dissolution rate once the most rapidly dissolving basalt fines had been dissolved. This increase in $\delta^{30}Si$ throughout the experiment may also reflect changes in dissolution of different minerals in the basalt. Olivine weathers faster and typically has a lower $\delta^{30}Si$ than more slowly dissolving plagioclases. An increase of the $\delta^{30}Si$ could thus result from a reduction of the ratio of olivine to plagioclase dissolution, although this effect is assumed to be minor as we expect that $\delta^{30}Si$ of these two minerals are fairly close in value to each other with no more than a maximal 0.1 to 0.2‰ difference. Fernandez et al. (2021a) noted that Ge/Si typically responds slower than $\delta^{30}Si$. In correspondance with this work, we observed a lag in the onset of partitioning of Ge/Si relative to Si isotope fractionation (**Figure 9**). In conclusion, the throughout this experiment persistently lower $\delta^{30}Si$ and Ge/Si in leachate from basalt treatments and therefrom inferred continuous mineral weathering and clay precipitation show that $\delta^{30}Si$ and Ge/Si can provide an effective tool in the toolbox for monitoring EW, though further work is needed to exploit their full potential.

Although monitoring of $\delta^{30}Si$ and Ge/Si can give valuable insights in weathering dynamics, to prove that inorganic CDR occurs, both DIC and SIC need to be quantified. Quantitatively, DIC leaching only sequestered approximately 40 kg CO_2-eq ha^{-1} $(125\ days)^{-1}$ in our experiment (**Figure 6),** which can be linearly extrapolated to 117 kg CO_2-eq $ha^{-1}year^{-1}$. Note that linear extrapolation is likely not representing reality, as silicate dissolution typically retards in time. No significant SIC increase was observed after basalt

amendment (**Figure 2b).** A possible explanation for the lack of SIC detection is that background SIC heterogeneity hampered the detection of a small SIC increase (Vienne et al., 2022). If the observed 2 ton CO_2 ha^{-1} SCE reduction between treatment 'B' and 'S' (**Figure 6b**) was caused by carbonate precipitation, this would correspond to a 0.035% SIC (350 mgSIC/kg soil) increase. For comparison, the standard error on the SIC difference measured between these two treatments was 415 mgSIC/kg soil. It thus remains unclear whether the lack of a significant change in SIC represents a detection failure or whether SIC did effectively not increase in the basalt treatment.

Cation mass balancing can shine a light on whether cations were dissolved from primary minerals and on the retention of cations within the soil column. The increase in exchangeable base cations observed in our basalt treatments (**Table 5**) shows that substantial weathering occured in our experiment, despite the relatively low number of DIC efflux. In **Table 6**, an overview of leached and exchanged cations is given, and the weathering rate of basalt in this experiment is calculated. In addition, from moles of weathered cations, using the η factors discussed in section 2.7, we can calculate inorganic CDR equivalents. Following this approach, (over our 137 days long experiment) we calculate optimistic inorganic CDR equivalents of 1.09±0.22 ton CO_2 ha^{-1} ($\eta^{++} = 2$) and a more conservative value of 0.62±0.11 ton CO_2 ha^{-1} ($\eta^{++} = 1$).

The optimistic inorganic CDR equivalent estimate hinges on several assumptions, including the values of the η factors (discussed in section 2.7). A second assumption for our circumneutral soil is absence of degassing of dissolved HCO_3^- by protons (which decreases CDR in acid soils (Calabrese et al., n.d.; Dietzen & Rosing, 2023)). As pore water pH was above neutral, we expect such degassing to be relatively minor in our experiment. Thirdly, it is possible to weather silicates without CO_2 sequestration if the weathering acid is not H_2CO_3 (Taylor et al., 2020). We therefore implicitly assume that H_2CO_3 is the only weathering agent, as we did not provide additional N or S fertilizer

to soils (and thus expect a limited contribution of other inorganic acids such as HNO_3 or H_2SO_4). Last, we assume that weathered base cations do not end up in other soil pools, such as the reducible and oxidizable soil pool which were not accounted for here (Tessier et al., 1979). The calculated minimal weathering rate may thus be an underestimation of the actual dissolution rate and actual inorganic CDR equivalents.

In conclusion, while mineral weathering rates can be quantified relatively well using the cation mass-balance approach, the associated carbon sequestration or export is more uncertain. For comparison, the changes in cumulative SCE (relative to the control soil treatment 'S') are also shown in **Table 6.** Importantly, in basalt earthworm treatments (BA, BE and BEA) the calculated inorganic CDR equivalents were positive while the experimentally observed SCE (the CDR) was negative, suggesting that SOC stocks were affected by basalt weathering.

4.1.2 Organic CDR mechanism?

We infer that substantial alkalinity was generated in this experiment but retained in the solid phase without commensurate alkalinity (DIC) leaching and significant changes in SIC (**Table 6, Figure 2b and 3**). During this experiment**,** we observed a decrease in cumulative SCE of approximately 2 ton CO_2 ha^{-1} after basalt amendment in non-worm soil, of which the DIC increase can explain only 0.04 ton CO_2 ha^{-1}. Likewise, Taylor et al. (2020) amended an acid rain impacted forest amended with 3.44 ton ha^{-1} wollastonite and measured a SCE reduction of about 2 ton CO_2 ha^{-1} after 15 years, while inorganic CDR was calculated to be relatively low over the same period (<0.2 ton CO_2 ha^{-1}) (numbers are derived from Figure 5 in Taylor et al. (2020)). Hence, the question arises: Is the driver of our observed SCE reduction in the basalt ('B') treatment stabilization of organic C, rather than inorganic CDR?

803 Mechanistically, silicate weathering may affect SOM stocks by altering two
804 major mechanisms: SOM stabilization and SOM decomposition. Firstly,
805 SOM can be stabilized through association of organic matter with cations as
806 DOC is adsorbed by these cations and thus becomes unavailable for microbial
807 respiration (Camino-Serrano et al., 2018). Exchangeable base cations could
808 even serve as predictors for SOM evolution after silicate amendment. In this
809 context, a recent analysis of 5500 soil profiles concluded that exchangeable
810 calcium was a better SOM predictor than soil texture (Rasmussen et al.,
811 2018). It should be noted however, that this relationship performed best in
812 alkaline (water-limited) soils (Aridisols, Mollisols and Alfisols). In wetter
813 and more acidic soils, Al-oxyhydroxides emerged as a better predictor relative
814 to exchangeable Ca (Rasmussen et al., 2018). Basalt dissolution leads to the
815 formation of (hydr)oxides of Al and Fe (e.g. amorphous $Al(OH)_3$,
816 ferrihydrite), which have been found to enhance SOM stabilization (Li, Hu,
817 Li, & Li, 2023). Dissolution of multivalent cations (Fe, Al and Ca) could
818 inform about SOM evolution after agricultural basalt amendment. Given that
819 base cation exchange was significantly increased here and given the well-
820 established correlation (yet no causal relationship) between SOM and soil
821 CEC (Rowley et al., 2018; Solly et al., 2020), this could have been the
822 dominant mechanism for the SCE reduction observed in this experiment. Yet,
823 SOM stabilization is not the only mechanism by which silicate dissolution
824 can affect SOM stocks.
825
826 When silicates are added to acid soil, soil pH increases and thereby changes
827 the stability of SOM and DOC in soil water (Dietzen et al., 2018; Malik et al.,
828 2018; Taylor et al., 2020; Wang et al., 2021). In a recent short-term incubation
829 experiment, Yan et al. (2023) showed that wollastonite increased the SCE of
830 acid soils (pH 4.43-6.42), with a larger effect for more acidic soils. Klemme
831 et al. (2022) recently estimated that the potential CDR associated with
832 enhanced weathering is reduced by 18–60% in tropical peatlands (which are

acidic) due to increased SOM decomposition after pH increase. te Pas et al. (2023) observed a (non-significant) decrease in SOM after amendment of an acid (pH 5) sandy soil with olivine, basalt, anorthite and albite in a short term experiment without plants, indicating increased SOM decomposition. Most recently in a field experiment in the corn belt, Kantola et al. (2023) found consistently higher heterotrophic respiration for four years in a row in basalt amended soils relative to unamended soil. In the wollastonite amended forest investigated by Taylor et al. (2020), DOC export increased after silicate amendment. Also in our experiment, the increased leachate DOC in all basalt treatments indicates increased decomposition post silicate amendment. Besides from changes in pH, microbes could also be stimulated if limiting (micro)nutrients for microbial growth are supplied with basalt addition. As the control soil in our experiment had a pH>7, the pH effect was presumably relatively small here and decomposition enhancement could be due to the removal of a nutrient limitation. Note that in our experiment, DOC leached from a shallow soil column whereas in actual soils, this DOC could be stabilized and increase SOC at greater depth.

Overall, the basalt amendment did not cause detectable SOC changes. As with SIC pools, this is unsurprising given the short duration of the experiment, which makes it difficult to detect a small change in a large and heterogeneous SOM stock.

The observed changes in organic carbon dynamics emphasise the need to consider basalt effects on both SOM decomposition and stabilization. In the future, holistic modelling of SOM changes by incorporation of a suite of parameters (pH, exchangeable Ca, Al/Fe (hydr)oxides, soil texture, temperature, soil moisture, plant type) in earth system models such as the Orchidee-SOM module (Camino-Serrano et al., 2018) could provide a more robust prediction of potential SOC increases following basalt amendment.

4.1.3 Literature review of experimentally derived basalt weathering rates and inorganic CDR equivalents.

In **Table 8**, studies of basalt mesocosm experiments (<1 year duration) are listed and sorted from high to low inorganic CDR equivalent rate (ton CO_2 ton $rock^{-1}$ $year^{-1}$). It offers a comparison between experimental weathering rates (mWr) and inorganic CDR equivalents observed in diverse EW experiments that use various quantification methodologies.

The log mWr of all these mesocosm studies are about an order of magnitude lower than shake flask based values of Brantley et al. (2008) which are -11 to -10 at pH 7 to 8 (our experimental pH range). The timescale of these benchtop experiments is typically less than several tens of days, while in column experiments weathering rates can decrease up to two orders of magnitude within the first year (Amann et al., 2022). The study of Buckingham et al., (2022) was recently criticized by West et al. (2023), mainly due to data gaps, utilization of an alkaline soil, the low infiltration flux of 57 mm $year^{-1}$ and extrapolation of these specific conditions for the whole UK. Interestingly, in our study we also utilize an alkaline soil and relatively low infiltration flux (130 mm $year^{-1}$). Yet, the log mWr (-11.65 ± 0.09 mol TA m^{-2} basalt s^{-1}) in our work is several orders of magnitude larger than in the study of Buckingham et al. (2022). We suggest that this reflects the importance of quantifying weathered cations in the exchangeable soil phase, a pool that was neglected by Buckingham et al. (2022) and others.

Table 8: Inorganic CDR equivalents and weathering rates of several short-term (≤1 year duration) mesocosm studies using basalt rock, assuming a factor of η^{++}=2 and η^{+}=1 (1 mol CO_2 mol^{-1} TA). This table is sorted from a high to low experimental inorganic CDR equivalent rate. Values that were not directly copied from the referred manuscripts were derived by calculation and are indicated in italics.

Ref	Application rate Ton rock ha^{-1}	Time years	Inorganic CDR equivalents*** (1 mol CO_2 mol^{-1} TA) ton CO_2/ha	Inorganic CDR equivalent rate (1 mol CO_2 mol^{-1} TA) ton CO_2 ton^{-1} rock $year^{-1}$	Water flux mm $year^{-1}$	Log mWr Log mol TA m^{-2} basalt s^{-1}	Quantification method
Kelland et al. (2020)	100	*0.33*	*2.40 ± 1.68*	*0.073± 0.051*	*767* [a] *2103* [b]	*-11.15 ±0.27*	Plant+ Leachate+ Exchangeable pool cations
This work (B-S)	100	0.38	1.96 ± 0.62	*0.055 ± 0.017*	130[b]	- [**]	ΔSCE
Reynaert et al. (2023)	50	0.33	0.84±0.91	0.051 ± 0.055	1226 [b]	*-11.40* ± 0.47	Plant+ Exchangeable pool cations
This work (BEA-S)	100	0.38	1.75± 0.28	*0.047± 0.008*	130[b]	-11.44±0.07	leachate+ Exchangeable pool cations
Reershemius et al. (2023)	50	*0.64*	1.34 ± 0.53 (NPK fertilized)	*0.042±0.017*	*1290*b*	*-11.53*±0.17	TiCat
Vienne et al. (2022)	50	1	1.83	*0.037*	143 [a]	*-11.54*	Phreeqc simulation
This work (treatment B-S)	100	0.38	1.09 ± 0.22	*0.029± 0.006*	130[b]	-11.65±0.09	leachate+ Exchangeable pool cations
te Pas et al. (2023)	*92**	*0.18*	*0.4-1.6**	*0.025-0.099**	*2568*b*	*-11.34* to -10.73**	Leachate+ Soil cations
Reershemius et al. (2023)	50	*0.64*	0.80 ± 0.21 (NPK fertilized)	*0.025 ± 0.007*	*1290*b*	*-11.75*±0.11	Plant+ Leachate+ Exchangeable pool cations
Reershemius et al. (2023)	50	*0.64*	0.78 ± 0.47 (manure fertilized)	*0.024±0.015*	*1290*b*	*-11.76*±0.26	TiCat
te Pas et al. (2023)	*92**	*0.18*	*0.40**	*0.024**	*2568*b*	*-11.34**	ΔSIC
Kelland et al. (2020)	100	1	2.36	*0.024*	*767* [a] *2103* [b]	-11.64	Phreeqc simulation
te Pas et al. (2023)	*92**	*0.18*	*0.4-1.6**	*0.025-0.099**	*2568*b*	*-11.34* to -10.73**	Leachate+ Soil cations
te Pas et al. (2023)	*92**	*0.18*	*0.40**	*0.024**	*2568*b*	*-11.34**	ΔSIC
Reershemius et al. (2023)	50	*0.64*	0.43 ± 0.19 (manure fertilized)	*0.013 ± 0.006*	*1290*b*	*-12.02*±0.19	Plant+ Leachate+ Exchangeable pool cations
Amann et al. (2022)	3206	*0 - 0.83*	*0-2.32* (saturated CO_2)	*0.027 to 0.001*	8000 [b]	-11 to -12.5 * (0-304 days)	Leachate cations
Amann et al. (2022)	3290	*0 - 0.83*	*0-0.24 (ambient CO_2)*	*0.003 to 9E-5*	8000 [b]	-12 to -13.5 * (0-304 days)	Leachate cations
Buckingham et al. (2022)	100	*0.67*	*0.014* ± 0.001	*14e-5 ± 1e-5*	57 [b]	*-14.21 ± 0.02*	Leachate cations
This work (BEA-S)	100	0.38	-2.00±1.20	*-0.056±0.034*	130[b]	- [**]	ΔSCE

[a] Infiltration flux, [b] irrigation flux. *Graphically estimated from reported figures. **As changes in SCE result not only from alkalinity release due to weathering, but also from changes in decomposition of SOM, no minimal Wr was calculated from the SCE change. A negative value for CDR means that higher CO_2 emissions relative to the control treatment were observed. *** If the quantification methodology is based on the ΔSCE, this column does not represent inorganic CDR equivalents, but an experimental CDR resulting from inorganic and organic C changes.

As such, this work thus adds to the growing awareness of the importance of exchangeable pool dynamics, as also emphasized by e.g. Reershemius et al. (2023). Whereas we found that the majority of released alkalinity (>98%) was released to the soil exchangeable pool, Kelland et al. (2020) even observed an alkalinity decrease in leachates. Despite that high irrigation rates (8000 mm $year^{-1}$) were used, cation retention might still have led to an underestimation of mineral dissolution rates in the basalt column experiments of Amann & Hartmann (2022). We argue that assessment of the soil exchangeable pool is crucial to quantify basalt weathering rates in soil systems, especially immediately following silicate application, as the system undergoes a transient adjustment to a new steady-state.

4.2 Basalt and earthworms

4.2.1 Basalt weathering rates and inorganic CDR in earthworms' presence

No positive basalt × earthworm interaction effect was found on the pH and elemental concentrations in the leachates. On the contrary, a negative earthworm × basalt interaction effect was found for K, Si and Mg concentrations in leachates. Earthworms slightly decreased leachate Ca, TA, DIC concentrations and cumulative DIC leaching in both basalt and control soil (**Figures 2, 3, 4 and 5).** Nonetheless, earthworms can still stimulate an alkalinity release if this alkalinity is retained in the soil system.

Earthworms can reduce soil water alkalinity through carbonate precipitation, clay formation, or increasing cation exchange. As we observed a tendency for a decrease rather than an increase in SIC, soil carbonate formation was unlikely stimulated by earthworm activity in our experiment. Our leachate

δ^{30}Si and Ge/Si data tentatively suggest that earthworms induced clay precipitation (Fernandez et al., 2021b)). This is consistent with Carpenter et al. (2007), who found production of clays by earthworms through XRD analysis. Since clays contain base cations, they serve as a relatively permanent alkalinity sink due to their slow weathering rates. An increase in clay precipitation will furthermore increase negatively charged sites that are available for cation exchange, which serves as a more transient alkalinity pool. As the capacity of a soil to hold cations in the exchangeable pool is finite, after a transient period alkalinity will be released to soil water again.

It was shown in our experiment that earthworms increased exchanged base cations (**Table 4)**. This increase matches the work of Wu et al. (2020), who found increased exchangeable base cations in earthworm casts. Note that the CEC of the SEA treatment decreased relative to treatment S, while the CEC of the BEA treatment increased relative to treatment B, pointing to a basalt × earthworm interaction effect on Ca, Mg and K exchange and suggesting that earthworms stimulated basalt dissolution. Earthworms have thus likely facilitated mineral dissolution in this experiment (see Log mWr in **Table 6**), without causing observable increases in SIC and DIC (the latter even decreased).

Note that the stimulation of weathering through anecic worm activity in this experiment could be different when compared to natural settings; our mesocosms (15cm depth) were shallower than the typical burrows of anecic earthworms which may have reduced the activity of anecic worms during this experiment. In future, earthworm effects could be tested under more realistic conditions, including deeper soils as well as vegetation. In any case, in all treatments, on average over 50% of anecic earthworms survived and were active at least in the first weeks of the experiment, as we observed that *Acer* leaves (**Figure 1a**) were dragged into the soil only in anecic earthworm mesocosms (**Supplementary Figure 2**).

4.2.2 Earthworms and SOC: short-term respiration increase versus long-term SOM stabilization?

During our short-term experiment, earthworms increased SCE in both control soil and basalt soil mixtures (**Figure 6b**). SCE was even stimulated more in basalt-earthworm mesocosms, despite the higher calculated weathering rate (see **table 6 and 8**). According to Zhang et al. (2013), heterotrophic respiration increases in the presence of earthworms because of higher microbial activity and mineralization of SOC in the gut of earthworms.

On the other hand, earthworms can also increase production of microbial necromass, which can stimulate formation of stable mineral associated organic matter (Angst et al., 2022). Also the increased release of cations by earthworm-accelerated weathering can stimulate organic matter stabilization. Shipitalo and Protz (1988) gathered indirect evidence that calcium, and to a lesser extent magnesium, are involved in the clay-polyvalent cation-organic matter linkages. By stimulating weathering and release of base cations, earthworms may thus enhance stabilization of SOM. The negative earthworm effect on DOC leaching supports this postulation. We infer that within the timescale of this short-term experiment earthworm-induced mineralization of SOC must have been larger than SOC stabilization by earthworms, such that no net carbon sequestration through earthworm activity was observed. Over longer timescales, however, increasing SOC stabilization may reverse this trend and lead to a net increase of SOC.

4.3 Influence of basalt on earthworm survival

In this experiment, an average earthworm survival rate between 52-63% and 52-70% was observed for anecic and endogeic worms respectively. No significant changes in survival of anecic or endogeic earthworms were observed after basalt amendment (**Table 7**), even though pH in basalt amended mesocosms rose up to ~8.5. Application of basalt (which increases bioavailable Ni, but below environmental standards (Vienne et al., 2022))

rather than ultramafic rocks such as dunite (which contain more Ni and Cr (Amann et al., 2020)) is expected to limit heavy metal contamination risk. *Apporectodea calignosa* and *Lumbricus* species are naturally occurring in basaltic soils, for example in Iceland (Sigurdsson & Gudleifsson, 2013), suggesting that these earthworms can thrive in the environment that we created in this experiment.

4.4 Recommendations for CDR monitoring in EW studies

This study provides valuable insights in basalt EW dynamics, notwithstanding that MRV (monitoring, reporting and verification) of EW remains challenging and the calculated inorganic CDR equivalents of 0.62 ton CO_2 ha^{-1} after 137 days (cation based estimate with $\eta^{++} = 1, \eta^{+} = 1$) comes with a series of assumptions and an uncertainty of 18%. We make the following recommendations for future monitoring of EW studies:

Firstly, in previous studies SIC was calculated as the difference between total soil C (TC) and SOC (SIC =TC-SOC), where SOC was quantified after acid digestion (Kelland et al., 2020; Vienne et al., 2022). Here, we measured SIC after removing organic matter through LOI to circumvent SOC heterogeneity from hampering inorganic C determination. Nevertheless, SIC heterogeneity remained substantial compared to the relatively small SIC increase from EW. To overcome this SIC heterogeneity issue in future EW experiments, acid control soils with SIC close to 0% could be selected (e.g. (tropical) soils) for short term studies (as was done by te Pas et al. (2023)) and larger application rates of silicate could be used in order to raise pH beyond the threshold for oversaturation of carbonates. Although such an experiment would be scientifically interesting, increasing application rates above 100 ton ha-1 is practically challenging from an agronomic point of view. In addition, as discussed in section 4.1.2, employment of acid soils for EW comes with the disadvantages of elevated bicarbonate degassing and SOM decomposition

after pH increase as argued by Dietzen et al. (2018) and more recently by Dietzen & Rosing (2023).

A second insight is that SCE monitoring can be a valuable tool that includes (in)organic effects and thus gives a more complete evaluation of the CDR through EW. In our case, SCE monitoring of bare soils allows to measure the resulting effect on inorganic CDR, SOM stabilization and SOM decomposition rates. SOM decomposition was found to be increased by silicate amendment in various studies that amended acid soils (Dietzen et al., 2018; Yan et al., 2023). Further research is needed to investigate under what conditions SOM decomposition decreases or increases after silicate amendment (e.g. by assessing activity of decomposing enzymes (peroxidases and (hemi)cellulases)).

Thirdly, we emphasise the importance of base cation monitoring. In future research, base cation monitoring of leachate water could be complemented with assessments of the soil exchangeable pool, but also in other soil pools (reducible, oxidizable soil pools, which were not assessed here). Such in-depth assessments can further improve our understanding of actual silicate weathering rates, the fate of weathering products and their long-term effects on SIC and SOC in EW systems. In conclusion, monitoring SIC changes in low background SIC soils, SCE, decomposition enzyme activity and base cations in all abovementioned soil pools could deliver robust data to pinpoint the rate and mechanism of C sequestration through EW using basalt rock.

5. Conclusions

In our lab mesocosm experiment, basalt addition to bare soils significantly increased leachate pH, Ca, Mg, TA and DIC. Basalt increased DIC export (inorganic CDR) only by about 40 kg CO_2 ha^{-1} over the course of the experiment (about 4 months). Despite low DIC leaching, soil water δ30Si and Ge/Si were always lower in basalt treatments than in mesocosms without

basalt addition, indicating that mineral weathering and clay precipitation took place and that δ30Si and Ge/Si can provide an effective tool in the toolbox for monitoring EW.

Although only low inorganic CDR was detected (note that failure of detection of an SIC change could still be due to soil carbonate heterogeneity), basalt addition decreased the soil CO_2 efflux in non-worm soils by approximately 2 ton CO_2 ha^{-1} within this experimental period, suggesting an organic CDR mechanism (SOC stabilization through cation association). Simultaneously, DOC in soil water increased post-basalt amendment, which indicates stimulation of decomposition of soil organic matter. Focussing only on DIC export and SIC may underestimate CDR if organic CDR mechanisms are at play. Effects of EW on organic carbon dynamics require further investigation to understand and quantify these effects.

Calculations based on changes in exchangeable cations revealed substantial weathering rates (>10^{-12} mol total alkalinity (TA) m^{-2} s^{-1}) which are over two orders of magnitude higher compared to the mWr calculated in earlier EW work in alkaline soil which did not take the exchangeable cation fraction into account. Leached alkalinity was negligible compared to cations retained in the columns' exchangeable fraction. Based on cation balancing, we estimate inorganic CDR equivalents between 0.62±0.11 and 1.09±0.22 ton CO_2 ha^{-1} in a more pessimistic and the most optimistic scenario, respectively. In conclusion, monitoring of cation exchange was crucial for quantifying inorganic CDR equivalents.

Earthworms decreased DIC export and did not seem to increase SIC which suggests that earthworms did not stimulate inorganic C sequestration. Although at first glance lower DIC export in earthworm treatments suggested reduced weathering rates, the increase in exchangeable cations shows that

earthworms increased weathering rates and the reduced DIC export was most likely due to promoted alkalinity retention by the solid phase (soil exchangeable pool). The earthworm-induced increase in exchangeable bases may furthermore stabilize organic matter in the long term. Nonetheless, increase of cumulative soil CO_2 efflux by earthworms was stronger in basalt relative to control soil mesocosms, which shows that stimulation of respiration by earthworms and their gut microbiota dominated over potential organic matter stabilization in the short term. In conclusion, earthworms with access to basalt did not increase CDR (and even stimulated SCE) within the timeframe of this experiment, yet earthworms are expected to have stabilized SOC through increasing weathering and base cation exchange.

Acknowledgements

We thank Mariana Rodriguez for measurement of soil CO_2 efflux and Nele Rodts for assisting in leachate sampling. In addition, we thank Anne Cools and Anke De Boeck for ICP-OES analyses and Miguel Portillo Estrada for elemental CN analysis. We thank Erik Verbruggen for the interesting discussions and assistance with designing graphical images. Josi Holtz and Daniel Frick are thanked for the smooth operation of the HELGES laboratory, and PJF acknowledges support from the GFZ 'Discovery' Fund. This research was supported by the Research Foundation— Flanders (FWO) [1S06323N] and by the Research Council UAntwerpen - Small Research Grants BOF 2021 [FFB210047]. Finally, we thank the EU Horizon 2020 BAM (bio-accelerated mineral weathering) project and the UPSURGE project for funding basalt enhanced weathering research.

Data availability

The original contributions presented in the study are included in the Supplementary Material, further inquiries can be directed to the corresponding author. Raw data and calculations of the weathering rate and for comparing weathering rates of studies can be consulted at (https://zenodo.org/record/7899975#.ZFTxh3ZBxPY).

ORCID

Arthur Vienne: https://orcid.org/0000-0002-0690-2481

Patrick Frings: https://orcid.org/0000-0002-1012-0642

Sílvia Poblador: https://orcid.org/0000-0002-4975-9777

Laura Steinwidder: https://orcid.org/ 0000-0002-9229-1786

Jet Rijnders: https://orcid.org/0000-0001-7896-0659

Jonas Schoelynck: https://orcid.org/0000-0003-0166-280X

Olga Vinduskova: https://orcid.org/0000-0002-7060-2459

Sara Vicca: https://orcid.org/0000-0001-9812-5837

REFS

Amann, T., Hartmann, J., Hellmann, R., Pedrosa, E. T., & Malik, A. (2022). Enhanced weathering potentials—the role of in situ CO2 and grain size distribution. *Frontiers in Climate*, *4*. https://doi.org/10.3389/fclim.2022.929268

Amann, T., Hartmann, J., Struyf, E., De Oliveira Garcia, W., Fischer, E. K., Janssens, I., … Schoelynck, J. (2020). Enhanced Weathering and related element fluxes - A cropland mesocosm approach. *Biogeosciences*, *17*(1), 103–119. https://doi.org/10.5194/bg-17-103-2020

Angst, G., Frouz, J., Willem, J., Stefan, V. G., Knabner, I. K.-, & Eisenhauer, N. (2022). *Earthworms as catalysts in the formation and stabilization of soil microbial necromass*. (April), 4775–4782. https://doi.org/10.1111/gcb.16208

Barker, S. (2013). Dissolution of Deep-Sea Carbonates. In *Encyclopedia of Quaternary Science* (2nd ed., Vol. 2). https://doi.org/10.1016/B978-0-444-53643-3.00289-2

Beerling, D. J., Leake, J. R., Long, S. P., Scholes, J. D., Ton, J., Nelson, P. N., … Hansen, J. (2018). Farming with crops and rocks to address global climate, food and soil security /631/449 /706/1143 /704/47 /704/106 perspective. *Nature Plants*, *4*(3), 138–147. https://doi.org/10.1038/s41477-018-0108-y

Berner, A. R. (2004). The Phanerozoic Carbon Cycle: CO2 and O2. *Oxford University Press*, *5*(4), 1155–1156. https://doi.org/10.2136/vzj2006.0054br

Bertagni, M. B., & Porporato, A. (2022). The Carbon-Capture Efficiency of Natural Water Alkalinization: Implications For Enhanced weathering. *Science of the Total Environment*, *838*(March), 156524. https://doi.org/10.1016/j.scitotenv.2022.156524

Blouin, M., Hodson, M. E., Delgado, E. A., Baker, G., Brussaard, L., Butt, K. R., … Brun, J. J. (2013). A review of earthworm impact on soil function and ecosystem services. *European Journal of Soil Science*, *64*(2), 161–182. https://doi.org/10.1111/ejss.12025

Brantley, S. L., White, A. F., & Kubicki, J. D. (2008). Kinetics of water-rock interaction. In *Kinetics of Water-Rock Interaction*. https://doi.org/10.1007/978-0-387-73563-4

Brown, I. C. (1943). A rapid method of determining exchangeable hydrogen and total exchangeable bases of soils. *Soil Science*, Vol. 56, pp. 353–357. https://doi.org/10.1097/00010694-194311000-00004

Buckingham, F. L., Henderson, G. M., Holdship, P., & Renforth, P. (2022). Applied Geochemistry Soil core study indicates limited CO 2 removal by enhanced weathering in dry croplands in the UK. *Applied Geochemistry*, *147*(October), 105482. https://doi.org/10.1016/j.apgeochem.2022.105482

Bullock, L. A., Yang, A., & Darton, R. C. (2022). Kinetics-informed global assessment of mine tailings for CO2 removal. *Science of The Total Environment*, *808*, 152111. https://doi.org/10.1016/j.scitotenv.2021.152111

Calabrese, S., Wild, B., Bertagni, M. B., Bourg, I. C., White, C., Aburto, F., … Porporato, A. (n.d.). *Nano- to Global-Scale Uncertainties in Terrestrial Enhanced Weathering*. https://doi.org/10.1021/acs.est.2c03163

Camino-Serrano, M., Guenet, B., Luyssaert, S., Ciais, P., Bastrikov, V., De Vos, B., … Janssens, I. A. (2018). ORCHIDEE-SOM: Modeling soil organic carbon (SOC) and dissolved organic carbon (DOC) dynamics along vertical soil profiles in Europe. *Geoscientific Model Development*, *11*(3), 937–957. https://doi.org/10.5194/gmd-11-937-2018

Cardinal, D., Alleman, L. Y., De Jong, J., Ziegler, K., & André, L. (2003). Isotopic composition of silicon measured by multicollector plasma source mass spectrometry in dry plasma mode. *Journal of Analytical Atomic Spectrometry*, *18*(3), 213–218. https://doi.org/10.1039/b210109b

Carpenter, D., Hodson, M. E., Eggleton, P., & Kirk, C. (2007). Earthworm induced mineral weathering: Preliminary results. *European Journal of Soil Biology*, *43*(SUPPL. 1), 176–183. https://doi.org/10.1016/j.ejsobi.2007.08.053

Darwin, C. R. (1981). *The formation of vegetable mould, through the action of worms, with observations on their habits.* (J. Murray., Ed.). Retrieved from https://www.biodiversitylibrary.org/item/189473#page/7/mode/1up

Delvigne, C., Angeletti, B., Guihou, A., Basile-Doelsch, I., & Meunier, J. D. (2018). Reliable Determination of Ge in Solid Environmental Samples Using a Chemical Preparation Procedure Developed for Si Isotopes and ICP-MS Analysis. *Geostandards and Geoanalytical Research*, *42*(1), 139–149. https://doi.org/10.1111/ggr.12197

Desie, E., Van Meerbeek, K., De Wandeler, H., Bruelheide, H., Domisch, T., Jaroszewicz, B., … Muys, B. (2020). Positive feedback loop between earthworms, humus form and soil pH reinforces earthworm abundance in European forests. *Functional Ecology*, *34*(12), 2598–2610. https://doi.org/10.1111/1365-2435.13668

Dietzen, C., Harrison, R., & Michelsen-Correa, S. (2018). Effectiveness of enhanced mineral weathering as a carbon sequestration tool and alternative to agricultural lime: An incubation experiment. *International Journal of Greenhouse Gas Control*, *74*(January), 251–258. https://doi.org/10.1016/j.ijggc.2018.05.007

Dietzen, C., & Rosing, M. T. (2023). Quantification of CO2 uptake by enhanced weathering of silicate minerals applied to acidic soils. *International Journal of Greenhouse Gas Control*, *125*(March),

103872. https://doi.org/10.1016/j.ijggc.2023.103872

Doetterl, S., Berhe, A. A., Arnold, C., Bodé, S., Fiener, P., Finke, P., … Boeckx, P. (2018). Links among warming, carbon and microbial dynamics mediated by soil mineral weathering. *Nature Geoscience*, *11*(8), 589–593. https://doi.org/10.1038/s41561-018-0168-7

Dorn, R. I. (2014). Ants as a powerful biotic agent of olivine and plagioclase dissolution. *Geology*, *42*(9), 771–774. https://doi.org/10.1130/G35825.1

Dudhaiya, A., Haque, F., Fantucci, H., & Santos, R. M. (2019). Characterization of physically fractionated wollastonite-amended agricultural soils. *Minerals*, *9*(10). https://doi.org/10.3390/min9100635

Fernandez, N. M., Perez-Fodich, A., Derry, L. A., & Druhan, J. L. (2021a). A first look at Ge/Si partitioning during amorphous silica precipitation: Implications for Ge/Si as a tracer of fluid-silicate interactions. *Geochimica et Cosmochimica Acta*, *297*, 158–178. https://doi.org/10.1016/j.gca.2021.01.007

Fernandez, N. M., Perez-Fodich, A., Derry, L. A., & Druhan, J. L. (2021b). A first look at Ge/Si partitioning during amorphous silica precipitation: Implications for Ge/Si as a tracer of fluid-silicate interactions. *Geochimica et Cosmochimica Acta*, *297*, 158–178. https://doi.org/10.1016/j.gca.2021.01.007

Frings, P. J., De La Rocha, C., Struyf, E., van Pelt, D., Schoelynck, J., Hudson, M. M., … Conley, D. J. (2014). Tracing silicon cycling in the Okavango Delta, a sub-tropical flood-pulse wetland using silicon isotopes. *Geochimica et Cosmochimica Acta*, *142*, 132–148. https://doi.org/10.1016/j.gca.2014.07.007

Frings, P. J., Schubring, F., Oelze, M., & von Blanckenburg, F. (2021). Quantifying biotic and abiotic Si fluxes in the Critical Zone with Ge/Si ratios along a gradient of erosion rates. *American Journal of Science*, *321*(8), 1204–1245. https://doi.org/10.2475/08.2021.03

Georg, R. B., Reynolds, B. C., Frank, M., & Halliday, A. N. (2006). New sample preparation techniques for the determination of Si isotopic compositions using MC-ICPMS. *Chemical Geology*, *235*(1–2), 95–104. https://doi.org/10.1016/j.chemgeo.2006.06.006

Gerrits, R., Pokharel, R., Breitenbach, R., Radnik, J., Feldmann, I., Schuessler, J. A., … Schott, J. (2020). How the rock-inhabiting fungus K. petricola A95 enhances olivine dissolution through attachment. *Geochimica et Cosmochimica Acta*, *282*, 76–97. https://doi.org/10.1016/j.gca.2020.05.010

Hodson, M. E., Black, S., Brinza, L., Carpenter, D., Lambkin, D. C., Mosselmans, J. F. W., … Versteegh, E. A. A. (2014). Biology as an Agent of Chemical and Mineralogical Change in Soil. *Procedia Earth and Planetary Science*, *10*(0), 114–117. https://doi.org/10.1016/j.proeps.2014.08.039

Huang, W., González, G., & Zou, X. (2020). Earthworm abundance and functional group diversity regulate plant litter decay and soil organic carbon level: A global meta-analysis. *Applied Soil Ecology*, *150*(December 2019), 103473. https://doi.org/10.1016/j.apsoil.2019.103473

IPCC, 2021: Summary for Policymakers. In: Climate Change 2021: The Physical Science Basis. Contribution of Working Group I to the Sixth

Assessment Report of the Intergovernmental Panel on Climate Change [Masson-Delmotte, V., P. Zhai, A. Pirani, S.L. Connors, C. Péan, S. Berger, N. Caud, Y. Chen, L. Goldfarb, M.I. Gomis, M. Huang, K. Leitzell, E. Lonnoy, J.B.R. Matthews, T.K. Maycock, T. Waterfield, O. Yelekçi, R. Yu, and B. Zhou (eds.)]. In Press.

Jicong, H., Yanyun, Q., Guangqing, L., & Dong, R. (2005). The Influence of Temperature , pH and C / N Ratio on the Growth and Survival of Earthworms in Municipal Solid Waste. *International Commission of Agricultural Engineering*, *7*(12), 1–6. Retrieved from http://hdl.handle.net/1813/10443

Kantola, I. B., Blanc-, E., Michael, B., Elliot, D. M., Marklein, A., Moore, C. E., … Delucia, E. H. (2023). *Improved net carbon budgets in the US Midwest through direct measured impacts of enhanced weathering*. (May), 1–17. https://doi.org/10.1111/gcb.16903

Kelland, M. E., Wade, P. W., Lewis, A. L., Taylor, L. L., Sarkar, B., Andrews, M. G., … Beerling, D. J. (2020). Increased yield and CO2 sequestration potential with the C4 cereal Sorghum bicolor cultivated in basaltic rock dust-amended agricultural soil. *Global Change Biology*, *26*(6), 3658–3676. https://doi.org/10.1111/gcb.15089

Klemme, A., Rixen, T., Müller, M., Notholt, J., & Warneke, T. (n.d.). *enhanced weathering*. (2022), 1–9. https://doi.org/10.1038/s43247-022-00544-0

Knapp, W. J., & Tipper, E. T. (2022). The efficacy of enhancing carbonate weathering for carbon dioxide sequestration. *Frontiers in Climate*, *4*. https://doi.org/10.3389/fclim.2022.928215

Lavallee, J. M., Soong, J. L., & Cotrufo, M. F. (2020). Conceptualizing soil organic matter into particulate and mineral-associated forms to address global change in the 21st century. *Global Change Biology*, *26*(1), 261–273. https://doi.org/10.1111/gcb.14859

Li, Q., Hu, W., Li, L., & Li, Y. (2023). Interactions between organic matter and Fe oxides at soil micro-interfaces: Quantification, associations, and influencing factors. *Science of the Total Environment*, *855*(July 2022). https://doi.org/10.1016/j.scitotenv.2022.158710

Liu, D., Lian, B., Wang, B., & Jiang, G. (2011). Degradation of potassium rock by earthworms and responses of bacterial communities in its gut and surrounding substrates after being fed with mineral. *PLoS ONE*, *6*(12). https://doi.org/10.1371/journal.pone.0028803

Lubbers, I. M., Van Groenigen, K. J., Fonte, S. J., Six, J., Brussaard, L., & Van Groenigen, J. W. (2013). Greenhouse-gas emissions from soils increased by earthworms. *Nature Climate Change*, *3*(3), 187–194. https://doi.org/10.1038/nclimate1692

Maleri, R. A., Reinecke, A. J., & Reinecke, S. A. (2008). Metal uptake of two ecophysiologically different earthworms (Eisenia fetida and Aporrectodea caliginosa) exposed to ultramafic soils. *Applied Soil Ecology*, *38*(1), 42–50. https://doi.org/10.1016/j.apsoil.2007.08.010

Maleri, R., Reinecke, S. A., & Reinecke, A. J. (2007). *Growth and Reproduction of Earthworms in Ultramafic Soils*. *370*, 363–370. https://doi.org/10.1007/s00244-005-0132-6

Malik, A. A., Puissant, J., Buckeridge, K. M., Goodall, T., Jehmlich, N., Chowdhury, S., … Griffiths, R. I. (2018). Land use driven change in soil pH affects microbial carbon cycling processes. *Nature Communications*, *9*(1), 1–10. https://doi.org/10.1038/s41467-018-

05980-1

Mortlock, R. A., & Froelich, P. N. (1996). Determination of germanium by isotope dilution-hydride generation inductively coupled plasma mass spectrometry. *Analytica Chimica Acta*, *332*(2–3), 277–284. https://doi.org/10.1016/0003-2670(96)00230-9

Oelze, M., Schuessler, J. A., & Von Blanckenburg, F. (2016). Mass bias stabilization by Mg doping for Si stable isotope analysis by MC-ICP-MS. *Journal of Analytical Atomic Spectrometry*, *31*(10), 2094–2100. https://doi.org/10.1039/c6ja00218h

Rasmussen, C., Heckman, K., Wieder, W. R., Keiluweit, M., Lawrence, C. R., Berhe, A. A., … Wagai, R. (2018). Beyond clay: towards an improved set of variables for predicting soil organic matter content. *Biogeochemistry*, *137*(3), 297–306. https://doi.org/10.1007/s10533-018-0424-3

Reershemius, T., Kelland, M. E., Davis, I. R., D'Ascanio, R., Kalderon-Asael, B., Asael, D., … Planavsky, N. J. (2023). *A new soil-based approach for empirical monitoring of enhanced rock weathering rates*. Retrieved from http://arxiv.org/abs/2302.05004

Renforth, P. (2012). The potential of enhanced weathering in the UK. *International Journal of Greenhouse Gas Control*, *10*, 229–243. https://doi.org/10.1016/j.ijggc.2012.06.011

Renforth, Phil. (2019). The negative emission potential of alkaline materials. *Nature Communications*, *10*(1). https://doi.org/10.1038/s41467-019-09475-5

Reynolds, B. C., Aggarwal, J., André, L., Baxter, D., Beucher, C., Brzezinski, M. A., … Cardinal, D. (2007). An inter-laboratory comparison of Si isotope reference materials. *Journal of Analytical Atomic Spectrometry*, *22*(5), 561–568. https://doi.org/10.1039/b616755a

Rosenstock, N. P., Van Hees, P. A. W., Fransson, P. M. A., Finlay, R. D., & Rosling, A. (2019). Biological enhancement of mineral weathering by Pinus sylvestris seedlings - effects of plants, ectomycorrhizal fungi, and elevated CO2. *Biogeosciences*, *16*(18), 3637–3649. https://doi.org/10.5194/bg-16-3637-2019

Rowley, M. C., Grand, S., & Verrecchia, É. P. (2018). Calcium-mediated stabilisation of soil organic carbon. *Biogeochemistry*, *137*(1–2), 27–49. https://doi.org/10.1007/s10533-017-0410-1

Savage, P. S., Armytage, R. M. G., Georg, R. B., & Halliday, A. N. (2014). High temperature silicon isotope geochemistry. *Lithos*, *190–191*, 500–519. https://doi.org/10.1016/j.lithos.2014.01.003

Schuiling, R. D., & Krijgsman, P. (2006). Enhanced weathering: An effective and cheap tool to sequester CO 2. *Climatic Change*, *74*(1–3), 349–354. https://doi.org/10.1007/s10584-005-3485-y

Shipitalo, M. J., & Protz, R. (1988). Factors Influencing the Dispersibility of Clay in Worm Casts. *Soil Science Society of America Journal*, *52*(3), 764–769. https://doi.org/10.2136/sssaj1988.03615995005200030030x

Sigurdsson, B. D., & Gudleifsson, B. E. (2013). Impact of afforestation on earthworm populations in Iceland. *Icelandic Agricultural Sciences*, *26*(1), 21–36.

SKALAR. (2022). Sanseries Automated Wet Chemistry Analyzer -

Continuous Flow Analyzer (CFA). Retrieved from https://www.skalar.com/analyzers/automated-wet-chemistry-analyzers/

Solly, E. F., Weber, V., Zimmermann, S., Walthert, L., Hagedorn, F., & Schmidt, M. W. I. (2020). A Critical Evaluation of the Relationship Between the Effective Cation Exchange Capacity and Soil Organic Carbon Content in Swiss Forest Soils. *Frontiers in Forests and Global Change*, *3*(September), 1–12. https://doi.org/10.3389/ffgc.2020.00098

Taylor, L., Driscoll, C., Groffman, P., Rau, G., Blum, J., & Beerling, D. (2020). Increased carbon capture by a silicate-treated forested watershed affected by acid deposition. *Biogeosciences Discussions*, 1–29. https://doi.org/10.5194/bg-2020-288

te Pas, E. E. E. M., Hagens, M., & Comans, R. N. J. (2023). Assessment of the enhanced weathering potential of different silicate minerals to improve soil quality and sequester CO2. *Frontiers in Climate*, *4*. https://doi.org/10.3389/fclim.2022.954064

ten Berge, H. F. M., van der Meer, H. G., Steenhuizen, J. W., Goedhart, P. W., Knops, P., & Verhagen, J. (2012). Olivine weathering in soil, and its effects on growth and nutrient uptake in ryegrass (Lolium perenne L.): A pot experiment. *PLoS ONE*, *7*(8). https://doi.org/10.1371/journal.pone.0042098

Tessier, A., Campbell, P. G. C., & Bisson, M. (1979). Sequential Extraction Procedure for the Speciation of Particulate Trace Metals. *Analytical Chemistry*, *51*(7), 844–851. https://doi.org/10.1021/ac50043a017

Van Bemmelen, J. (1890). Über Die Bestimmung Des Wassers, Des Humus, Des Schwefels, Der in Den Colloïdalen Silikaten Gebundenen Kieselsäure, Des Mangans U. S. W. Im Ackerboden. *Die Landwirthschaftlichen Versuchs-Stationen*, *37*, 279–290.

Verbrigghe, N., Leblans, N. I. W., Sigurdsson, B. D., Vicca, S., Fang, C., Fuchslueger, L., … Janssens, I. A. (2022). Soil carbon loss in warmed subarctic grasslands is rapid and restricted to topsoil. *Biogeosciences*, (December 2021), (in press).

Verbruggen, E., Struyf, E., & Vicca, S. (2021). Can arbuscular mycorrhizal fungi speed up carbon sequestration by enhanced weathering? *Plants People Planet*, *3*(5), 445–453. https://doi.org/10.1002/ppp3.10179

Versteegh, E. A. A., Black, S., & Hodson, M. E. (2014). Environmental controls on the production of calcium carbonate by earthworms. *Soil Biology and Biochemistry*, *70*, 159–161. https://doi.org/10.1016/j.soilbio.2013.12.013

Vicca, S., Goll, D., Hagens, M., Hartmann, J., Janssens, I. A., Neubeck, A., … Verbruggen, E. (2022). Is the climate change mitigation effect of enhanced silicate weathering governed by biological processes? *Global Change Biology*, (July), 1–16. https://doi.org/10.1111/gcb.15993

Vidal, A., Watteau, F., Remusat, L., Mueller, C. W., Nguyen Tu, T. T., Buegger, F., … Quenea, K. (2019). Earthworm cast formation and development: A shift from plant litter to mineral associated organic matter. *Frontiers in Environmental Science*, *7*(APR), 1–15. https://doi.org/10.3389/fenvs.2019.00055

Vienne, A., Poblador, S., Portillo-estrada, M., Hartmann, J., Ijiehon, S., Wade, P., & Vicca, S. (2022). *Enhanced Weathering Using Basalt Rock Powder : Carbon Sequestration , Co-benefits and Risks in a*

Mesocosm Study With Solanum tuberosum. *4*(May), 1–14. https://doi.org/10.3389/fclim.2022.869456

Wang, Y., Yao, Z., Zhan, Y., Zheng, X., Zhou, M., Yan, G., … Butterbach-Bahl, K. (2021). Potential benefits of liming to acid soils on climate change mitigation and food security. *Global Change Biology*, *27*(12), 2807–2821. https://doi.org/10.1111/gcb.15607

Wen, S., Wang, J., Li, Y., & Shao, M. (2022). Effects of anecic earthworms on runoff and erosion on the slope with soil from the Loess Plateau under a rainfall simulation experiment. *Agricultural Water Management*, *259*(June 2021), 107230. https://doi.org/10.1016/j.agwat.2021.107230

West, L. J., Banwart, S. A., Martin, M. V., Kantzas, E., & Beerling, D. J. (2023). Making mistakes in estimating the CO2 sequestration potential of UK croplands with enhanced weathering. *Applied Geochemistry*, *151*(January), 105591. https://doi.org/10.1016/j.apgeochem.2023.105591

Wiesmeier, M., Urbanski, L., Hobley, E., Lang, B., von Lützow, M., Marin-Spiotta, E., … Kögel-Knabner, I. (2019). Soil organic carbon storage as a key function of soils - A review of drivers and indicators at various scales. *Geoderma*, *333*(November 2017), 149–162. https://doi.org/10.1016/j.geoderma.2018.07.026

Wild, B., Gerrits, R., & Bonneville, S. (2022). The contribution of living organisms to rock weathering in the critical zone. *Npj Materials Degradation*, *6*(1). https://doi.org/10.1038/s41529-022-00312-7

Winnick, M. J., & Maher, K. (2018). Relationships between CO2, thermodynamic limits on silicate weathering, and the strength of the silicate weathering feedback. *Earth and Planetary Science Letters*, *485*(January), 111–120. https://doi.org/10.1016/j.epsl.2018.01.005

Wolf-Gladrow, D. A., Zeebe, R. E., Klaas, C., Körtzinger, A., & Dickson, A. G. (2007). Total alkalinity: The explicit conservative expression and its application to biogeochemical processes. *Marine Chemistry*, *106*(1-2 SPEC. ISS.), 287–300. https://doi.org/10.1016/j.marchem.2007.01.006

Wood, C., Harrison, A. L., & Power, I. M. (2022). ur na l P re r f. *Applied Geochemistry*, 105511. https://doi.org/10.1016/j.apgeochem.2022.105511

Wu, J., Zhang, C., Xiao, L., Motelica-Heino, M., Ren, Z., Deng, T., & Dai, J. (2020). Impacts of earthworm species on soil acidification, Al fractions, and base cation release in a subtropical soil from China. *Environmental Science and Pollution Research*, *27*(27), 33446–33457. https://doi.org/10.1007/s11356-019-05055-8

Yan, Y., Dong, X., Li, R., Zhang, Y., Yan, S., Guan, X., … Zhang, W. (2023). Catena Wollastonite addition stimulates soil organic carbon mineralization : Evidences from 12 land-use types in subtropical China. *Catena*, *225*(February), 107031. https://doi.org/10.1016/j.catena.2023.107031

Zhang, W., Hendrix, P. F., Dame, L. E., Burke, R. A., Wu, J., Neher, D. A., … Fu, S. (2013). Earthworms facilitate carbon sequestration through unequal amplification of carbon stabilization compared with mineralization. *Nature Communications*, *4*, 1–9. https://doi.org/10.1038/ncomms3576

Ziegler, K., Chadwick, O. A., Brzezinski, M. A., & Kelly, E. F. (2005).

Natural variations of δ30Si ratios during progressive basalt weathering, Hawaiian Islands. *Geochimica et Cosmochimica Acta*, *69*(19), 4597–4610. https://doi.org/10.1016/j.gca.2005.05.008